1

Substrate Preparation

1.1 Introduction

Deposits must adhere well to the substrates in the *chosen places*. The adhesion of a deposit is achieved by several physico-chemical mechanisms in contact between the deposit material and that of the substrate (discussed in detail in Chapter 4). All these mechanisms work, however, under the condition that the surface of this contact is clean. A ***clean surface*** can be defined after Mattox [1] as "a surface which contains no significant amount of undesirable material." The degree of required property varies with the deposition technique.

Consequently, the films obtained with *atomistic deposition* methods require high level of cleanliness so that the atoms or molecules of a deposit that condense on the surface do not come into contact with a very fine of dust or another contamination of a small dimension. The thick coatings obtained by *granular deposition* techniques use generally molten particles to build up the deposit, and the required degree of purity is relatively smaller than that required for thin films. However, the adhesion of such coatings to the substrate must be improved by the surface activation. Similarly, the surfaces of the substrates coated by *bulk deposition* methods are molten to enable coating material particles to be injected what lowers considerably the purity requirement.

The impurities, which can be found on the surfaces of substrates and the methods of their cleaning, depend also on the material. The types of material determine the type bonding and the nature contaminants, which is different for metal and alloys, ceramics, and polymers. Consequently, the typical substrates materials used in different deposition methods are shortly described.

The purity of a surface of a substrate can be achieved by removing the contamination by following methods:

- chemical (chemical attack, dissolution of impurities, etc.);
- physical which is realized by:
  - high temperature treatment;
  - *mechanical cleaning* using particles abrasion (grit blasting) or water jet *ultrasonic cleaning*;
  - *photonic cleaning* using laser or by polychromatic *uv* radiation;
  - *plasma cleaning* using arc or ion bombardment.

Physical Deposition Methods for Films and Coatings, First Edition. Lech Pawłowski.

The films or coatings should be deposited in chosen places on the substrate. The places must be somehow defined. The chapter describes patterning using ***lithography*** and ***direct patterning***. The *lithography* is a classical masking technique, which has been used in semiconductor industry since many decades. It can be applied directly on the substrate if high resolution is desired. Alternatively, this technique can be applied to manufacture the *stencil masks* which, although less precise, can be used multiple times also in granular deposition methods. The resolution photolithographic masks depend on the *illumination sources* leading to the photo-polymerization (*uv* – radiation, X-rays, *e*-beam, *i*-beam, etc.). The *direct patterning* enables maskless protection of the substrates using different mechanisms such as oxidation of thin metal films or thermal decomposition of polymers [2]. This kind of patterning may be used in technology of atomistic films. Some granular coatings, such as cold-gas spraying method (*CGSM*), enable also direct patterning of sprayed coating.

The methods of cleaning methods are often empirical and are a part of a deposition procedure. The surface should be clean to obtain well-adhering film or coating. However, this condition is necessary but not sufficient to obtain a good adhesion of a deposit. Sometimes the surface has to be activated prior to deposition processes. In particular, the surface activation is essential to obtain adhesion of granular deposits. This results from the fact that one of principal adhesion mechanisms is the mechanical attachment of liquid particles to the top parts of surface irregularities. Consequently, it is necessary to roughen the surface by, e.g. grit-blasting. On the other hand, a surface of a polymer substrate must be activated in order to apply any deposit. Such activation can be done using plasma by, e.g. corona discharge. Finally, the application of a bond-coat can also be seen as activation of a substrate.

Surface cleaning and their activation are part of the pre-treatment of a substrate prior to film or coating deposition. Very often, the deposition does not directly follow the pre-treatment, and the substrate remains sometime in contact with the ambient atmosphere, which may result in a re-contamination. The appropriate storage of pre-treated substrates may avoid such recontamination.

1.2 Surfaces of Different Types of Substrates (Metals and Alloys, Ceramics, Polymers)

The substrates are made of different materials depending on the deposition method. Atomistic techniques are applied for the deposition of metals and alloys, ceramics (oxides, nitrides, carbides), carbon and polymers films on metals and alloys, ceramics (oxides and carbides), semiconductors, and polymers. The granular techniques are most frequently applied to the coatings of metals and alloys, ceramics (mainly oxides and carbides), and more seldom polymers and the composites (oxides – metals, polymers – oxides). The used substrates are mainly metals, alloys, and more seldom ceramics and polymers. Finally, the bulk deposition techniques are applied for coatings of metals and alloys, ceramics (oxides and carbides), and their composites (oxides – metals by the hard-phase dispersion technique) on the substrates of metals and alloys. Substrates used in bulk coatings techniques require less preparation than in others. Consequently, this chapter describes briefly metals/alloys, ceramics/glasses, and polymers and their physicochemical properties which play a role in films and coatings deposition.

Films and coatings are deposited onto surface of materials. Surfaces have different properties than bulk material. It results from the forces acting on the atoms/molecules (see Fig. 1.1). The surface is in contact with other phase (liquid or gas), and the forces of interaction with the atoms or molecules are much smaller than those in the solid. The difference between the forces can be described as ***surface energy***, being equal to the difference between the energy of all atoms/molecules in the surface and that they may have inside the solid [3].

The *surface energy* can be interpreted as a work of displacing the atoms/molecules (called particles thereafter) from the solid bulk to its surface. This energy decreases with the temperature[1] and is equal to zero at ***critical temperature*** and ***pressure*** when the phase solid and liquid/gas disappear and, consequently, the solid surface disappears too. The *surface energy* depends also on its morphology. The surfaces are seldom flat and have frequently peaks or corners shown in Fig. 1.2. The particles have lower number of neighbors, and the *surface energy* is greater. Consequently, the reactivity of the rough surface is greater than that of flat ones, and the corners and edges include more products of reaction than other places on the surface.

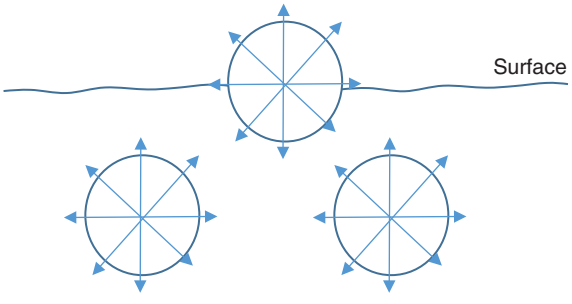

Figure 1.1 Forces acting on atoms or molecules on the surface and in the bulk of a solid. *Source:* Adapted from Burakowski and Wierzchoń [3].

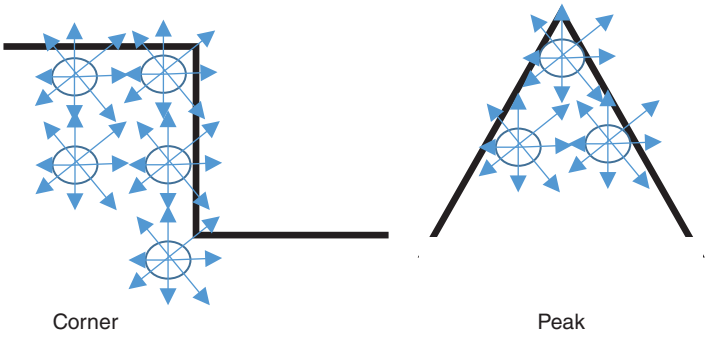

Figure 1.2 Forces acting on the surface including a corner and a peak.

1 For example, the *surface energy* of solid alumina at temperature of 2123 K is 0.905 N/m and of liquid alumina having temperature 2353 K is 0.7 N/m [4]

The particles on the solid surface are fixed and do not move. However, in many cases, the surface is heated and its temperature increases. At the temperatures close to the melting point, the particles can move and the number of irregularities decreases. It results from the tendency to decrease the surface area, as in the liquids. This tendency is an effect of interaction of the particles inside the body with the particles on its surface and is described by ***surface tension***, γ. This parameter can be described by the ratio of internal free energy, E, and the surface area, A, as:

$$\gamma = \frac{\partial E}{\partial A} \tag{1.1}$$

The *surface tension* is frequently used in describing the liquids. It reduces their surface area and makes the droplet spherical. It can be defined, for the solids after Kingery et al. [4], as the work done in creating new surfaces by adding new particles to this surface.

The real bodies are manufactured in different ways, and their surfaces result from the manufacturing process, which may be divided roughly as: (i) mechanical (grinding, polishing, etc.); (ii) thermal (casting, heating, etc.); and (iii) chemical (alloying, chemical reaction, etc.). Each of these processes is in practice associated with physical and chemical phenomena as diffusion, crystallization, melting, solidification, adsorption, and many others. The state of a surface may be roughly described using properties/data:

- thermodynamical (*surface energy, surface tension*, temperature, etc....);
- mechanical (roughness, hardness, parameters describing elasticity, fracture, or stresses, etc.);
- chemical (chemical composition and crystal phases, etc.);
- physical (thermal or electrical conductivity, thermal expansion, optical emission, etc.).

Moreover, many of these properties change with the distance from the surface, and a couple of zones having different thickness (e.g. 3–5 zones models following [4]) can be distinguished. Finally, the manufacturing processes and the properties of surface depend strongly on the properties of the bulk material. That is why the useful information will be described for three types of materials: metals and alloys, ceramics, and polymers.

1.2.1 Metals and Alloys

The volume near to the metallic surface submitted to a thermomechanical treatment may include many zones depending on the kind of treatment, the temperature of the treatment, and its duration. To give an example, the 5-zone model, presented in Fig. 1.3, includes the following zones [3]:

- zone I being a *near-surface zone* in direct contact with the environment and includes some atoms and ions coming from the atmosphere around and from the surface of solids being in contact and the thickness of this zone is smaller than 1 nm;
- zone II called also *directed grains zone* includes the crystal grains deformed in a similar direction after the treatment;
- zone III known also as *thermal effects zone* which includes the grains influenced (size, phase composition, etc.) by temperature, and the thickness depends on temperature and on time of the treatment;

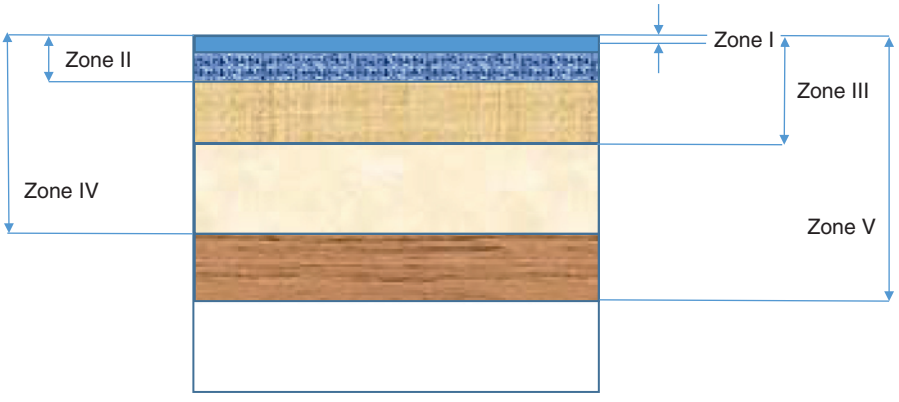

Figure 1.3 Five-zones of metallic surface after mechanical or thermomechanical treatment. Description of zones is in the text. *Source:* Adapted from Burakowski and Wierzchoń [3].

- zone IV is *textured grains zone* which includes the grains having similar crystallographic texture;
- zone V is known also as *crush zone* deformed plastically at thermomechanical treatment, and the thickness may reach a few to a hundred μm.

The metal or alloy surface in contact with atmosphere may adsorb species. The adsorbing surface is called ***adsorbent***, and the adsorbed species are called ***adsorbate***. The mechanism of adsorption may be [3, 5]: (i) physical, in which the species are attached by relatively weak ***van der Waals forces***; or, (ii) chemical, in which the *adsorbent* enters in reaction with *adsorbate*. Some authors add ***condensation adsorption*** in which the adsorbed gases transform in liquid. Such condensation may occur at the pressure, which is greater than a critical for given temperature [3]. Finally, ion-exchange adsorption is possible, in which the ions presented on the solid surface are replaced by the ions from the gas phase [5]. The possible adsorption mechanisms and different ***isotherm models*** enable predicting the adsorption amount on a solid surface at constant temperature.

Metals and alloys are generally highly reactive, and the contact with open atmosphere leads to a formation of oxides or nitrides. The oxidation of metallic surface in such atmosphere is more probable than its nitriding. This results from thermodynamic properties of oxides and nitrides. The Gibbs free energy of formation of oxides is much more negative as shown in Table 1.1. The comparison of the mass of formed oxides or nitrides depends however on the diffusion of oxygen and nitrogen across the oxide or nitride film. The dense oxide films as those of Al_2O_3 remain much thinner by forming an efficient barrier for oxygen diffusion [7].

The oxidation of a metal starts formation of metal ion and electron(s), which diffuse through the oxide film to meet and to enter in reaction with oxygen from air. The sketch of formation of oxide film oxidation in 1-D is shown in Fig. 1.4. The reaction occurring in the film is:

$$M + O \rightarrow MO \tag{1.2}$$

Table 1.1 Standard free energy of formation of some oxides and nitrides[a].

Oxides		Nitrides	
Compound	**$\Delta_f G°_{298}$ (kJ/mol)**	**Compound**	**$\Delta_f G°_{298}$ (kJ/mol)**
Al_2O_3	−1573	AlN	−287
CrO_3	−506.3	CrN	−92
Fe_2O_3	−744.8	Fe_2N	+12.6
CuO	−128.4	Cu_3N	+74.5
MoO_3	−669.4	Mo_2N	−50.2
TiO_2	−891.2	TiN	−309.2

[a] More negative Gibbs energy means that reaction is more probable. Positive energy of Gibbs means that the compound is stable. *Source:* Adapted from Elder et al. [6].

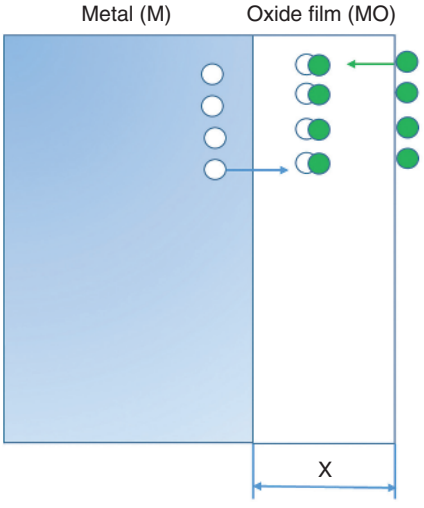

Figure 1.4 Mechanism of parabolic growth of oxide film.

The oxidation can be accompanied with three possible diffusions, namely those of [7]: (i) oxygen atoms (molecules) toward metal surface; (ii) metal atoms toward oxide film surface; (iii) electrons from metal substrate toward oxide film surface. The flux of each diffusing species results from its concentration gradient and can be described by ***Fick's first law***:

$$J = -D\frac{dC}{dx} \tag{1.3}$$

If we consider only oxygen, then the gradient of its concentration is equal simply to the ratio of its concentration to the film thickness, supposing that its concentration $C_{(O)} = 0$ at the metal surface:

$$\frac{dC_{(O)}}{dx} \approx \frac{C_{(O)}}{x} \tag{1.4}$$

Knowing that the velocity of oxide film growth, dx/dt is proportional to the flux of oxygen atoms, we may obtain the differential equation [6]:

$$\frac{\mathrm{d}x}{\mathrm{d}t} = -D\frac{C_{(O)}}{x} \tag{1.5}$$

The solution of the equation is $x^2 \sim t$ and shows that the square of oxide thickness is proportional to time of oxidation. This type of oxide growth is known as ***parabolic oxidation*** and describes the growth in continuous films. On the other hand, the growth of oxides films at high temperatures may lead to their fracturing because of the mismatch of thermal expansions coefficients of the metal and its oxide. This phenomenon may lead to the ***linear oxidation*** at which the oxide film thickness is proportional to oxidation time $x \sim t$. More details about oxidation mechanism can be found, e.g. in the textbook of Ashby and Jones [7].

The atoms well below the zone V (see Fig. 1.3) in the metals and alloys interact generally by metallic bonding (see Fig. 1.5). The valence electrons are not bound to any atom, and they may drift inside entire metal or alloy forming a "sea of electrons." The free electrons help in "gluing" of metal ions together and render metals and alloys good conductors of electricity and of heat. The bonding energy may reach 8.8 eV/atom for tungsten [8].

The atoms and ions in metals and alloys are arranged in the periodic network. Exceptionally, the rapid solidification may lead to the formation ***amorphous structure***, without any short- or long- distance order. The crystal structures can be described by geometry of ***unit cells***. There are, in total, seven crystal systems, and metals have frequently structures *FCC*, *BCC,* and *HCP* [8]. Most of crystalline solids are composed of small crystals rendering metals and alloys ***polycrystalline***. The crystal grains are in contact with each other by ***grain boundaries***. The boundaries weaken the bonding energy between atoms in neighboring grains. In addition, the diffusion through the boundaries is much easier than that through the crystals.

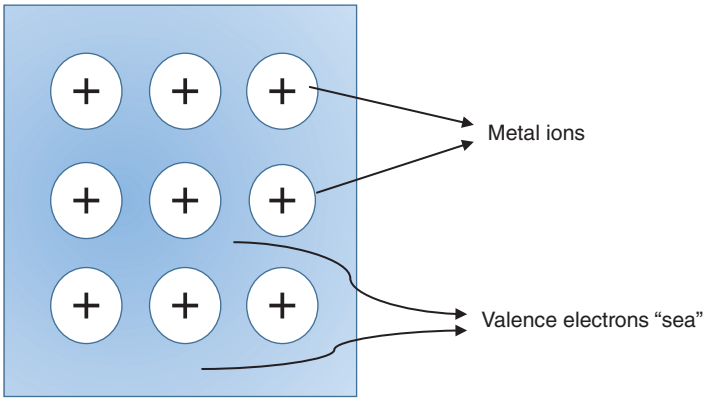

Figure 1.5 Metallic bonding showing metal ions and sea of valence electrons. *Source:* Adapted from Callister [8].

Table 1.2 Physicochemical and mechanical properties of some metals and alloys useful in surface preparation prior to films and coatings deposition [7, 9–12].

Metal or alloy	T_m, K	Elastic modulus, E, GPa	Time needed to obtain 1 mm thick oxide at temperature $0.7*T_m$, h
Al	933	69	Very long
Cr	2180	268	1600
Fe	1811	200	24
Cu	1358	117	25
Mo	2896	330	Very short
Ti	1941	114	<6
NiAl	1955	170	—
Stellite 6	1558–1683	237	—
Bronze	1223	96–120	—

The properties of metallic substrates, important for the preparation of films and coatings, include a few physicochemical and mechanical properties such as:

- melting point, helping in the choice the temperature of preparation treatment;
- oxidation resistance, some data concerning oxidation are discussed above (see Table 1.1 and Fig. 1.4);
- hardness, which renders the substrate activation by mechanical methods as sand-blasting is more or less difficult.

Table 1.2 is a collection of some useful data for typical metal and alloys. The melting point, T_m, is important to indicate the temperature, which can be used for the treatment prior to deposition of film and coatings. This temperature should be kept low for substrates of aluminum, copper, or *bronze*.

The modulus elasticity indicates the method that can be used to the substrate activation of substrate. Obviously, the substrate of molybdenum or chromium are hard to activate by mechanical methods, and chemical methods may be more useful. Finally, the oxidation activity determines time lapse between the substrate's surface activation and the film or coating deposition. This time should be short for molybdenum or titanium and longer for aluminum or chromium (which oxidizes rapidly, but thin oxide films are dense and do not grow up). This may also be useful to decide whether the activated substrates can be preserved for long periods in open or in an inert atmosphere.

1.2.2 Ceramics and Glasses

Ceramics and glasses can be defined as materials having strong covalent and ionic bonding. Examples of covalent ceramics are:

- different polymorphs of carbon, such as diamond, graphite, or fullerenes [8];
- compounds having structure similar to diamond, such as Si_3N_4 [13].

The ionic ceramic is composed of cations such as Al^{+3} or Ca^{+2} and anions as O^{2-}. The radius of anions, r_a, is generally greater than that of cations, r_c. The stability of ionic ceramic increases with the ratio of the radii r_c/r_a. If the ratio $r_c/r_a > 0.155$ then each cation is surrounded by, at least, three anions [8]. Stability concerns also an interaction between the ceramics surface and open atmosphere. As there are no chemical reactions of ceramics with oxygen or with nitrogen, this interaction is mainly physical and can be described by *surface energy*, *surface tension* (see Eq. (1.1)), adsorption, and diffusion.

The *surface energy* (see Table 1.3), which tends to have a possible low value, plays an important role in the distribution of impurities on the surface. The impurities arriving on the surface of ceramics will remain there more or less concentrated depending on their *surface tension*. Some values of *surface tensions* for liquids, which may be impurities, are collected in Table 1.4. The impurities having low *surface tension* would remain concentrated on the surface. Contrarily, those of high *surface tension* would tend to be less concentrated. The surface may lower its energy by adsorption of impurities. In the case of ionic crystals, their surfaces are filled with anions and cations and may attract ions, if there are any. The fractured ion crystal surface has high *surface energy* and attracts oxygen from air to lower this energy [4].

The surface of ceramics may be in contact with impurities being in gaseous and liquid phases. The contact with gaseous phase may be described by adsorption and diffusion. The contact with liquid phase needs an introduction of ***wetting***, which is generally analyzed for

Table 1.3 *Surface energy* of some ceramic materials and glasses [4, 14–16].

Ceramics	T_m, K	T, K	Surface energy, N/m
Al_2O_3	2327	1273	1.0
		2123	0.905
MgO	3073	298	1.0
$SiO_2 + 20$ wt.% Na_2O		1623	0.38
$SiO_2 + 13$ wt.% $Na_2O + 13$ wt. % CaO (liquid)			0.35
TiC	3430	1373	1.19
$CaCO_3$ (monocrystal)	1612	298	0.23

Table 1.4 *Surface tension* of some liquids having temperature of $T = 293$ K.

Liquid	γ, mN/m
Water	72.75
Ethanol	22.28
Pentane	15.7
Hexane	18.52

Source: Adapted from Snustad et al. [17].

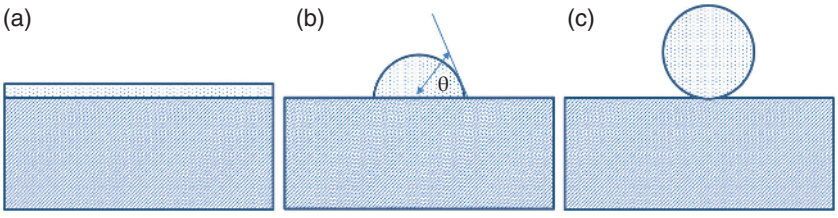

Figure 1.6 Behavior of liquid droplet on a solid surface: (a) spreading corresponding to $\theta = 0°$; (b) wetting corresponding to $\theta < 90°$; and (c) non-wetting corresponding to $\theta > 90°$ ($\theta = 180°$ in the Fig. 1.7c).

a liquid droplet on solid surface using angle θ as shown in Fig. 1.6. The droplet may spread entirely ($\theta = 0$). The wetting occurs for $\theta < 90°$ and non-wetting, for angle $\theta > 90°$. The *Young–Dupré* law enables predicting angle of wetting, θ, from *surfaces energies* of liquid and solid and from cohesion force of the liquid [18]. An important factor influencing wetting is surface roughness discussed, e.g. by Snustad et al. [17]

The crystal structure of ionic ceramics depends on the ratio of anions to cations and on number of anions. The anions, being much greater, can have a simple cubic structure (e.g. SiC) or *FCC* (e.g. MgO, $BaTiO_3$, or $MgAl_2O_4$). The silica and silicate structure is generally characterized by a tetrahedron in which every Si atom in the center is bonded by O being in the corners. Finally, covalent ceramics such as diamond, graphite, and fullerenes have the structure subsequently, *diamond cubic*, layers of hexagonally arranged carbon atoms and cluster of 60 carbon atoms, called C_{60} [8].

Ceramic materials are often manufactured from powders, which are sintered in temperatures lower than melting point. Consequently, such materials are polycrystalline and include some porosity. The glasses, being composed of silica and oxides of sodium, boron, or calcium among others, are generally amorphous. The electrical and mechanical properties of ceramics depend strongly on the porosity. In particular, the modulus of elasticity of porous ceramics modifies the modulus of no-porous material, E_0, in the following way [19]:

$$E = E_0\left(1 - c_1 P + c_2 P^2\right) \tag{1.6}$$

In the equation, the constants c_1 and c_2 depend on the shape of pores.

The ceramic materials may be conductors, semiconductors, and electrical isolators. This results from the electron energy gap between valence and conducting band, which can be at room temperature [4]:

- occupied, as in metals and in some oxides as CrO_2 or in TiO;
- partly occupied, as in semiconductors such as Si ($E_g = 1.1\,eV$) or GaAs ($E_g = 1.4\,eV$);
- empty, as in electric isolators as BN ($E_g = 5.9\,eV$) or Al_2O_3 ($E_g > 8\,eV$).

The elasticity modulus of some ceramic materials shows very high values for diamond and SiC (see Table 1.5). Another important property of these materials is their brittleness. The latter renders them hard to deform and to activate mechanically prior to the films and coatings deposition.

Table 1.5 Elasticity modulus for some ceramics [4, 20].

Material	Porosity, *P*, %	Elasticity modulus, *E*, GPa
Diamond		1164
SiC		469
TiC		310
Al_2O_3	5	365
ZrO_2 (stabilized)		151
BN		82.7
SiO_2 glass		72.5
Pyrex glass[a], SiO_2 + 12.6 wt. % B_2O_3 + 4.2 wt. % Na_2O + 2.2 wt. % Al_2O_3		70.0
Graphite	20	8.96

[a] Chemical composition corresponding to the equivalent glass *Corning 7740*. Diamond and pyrex glass are not porous

1.2.3 Polymers

Polymers are composed of hydrocarbons including ***macromolecules*** in which there are generally identical ***repeat units*** called also ***monomers***, such as ethylene, C_2H_4, or tetrafluoroethylene, C_2F_4. The *monomers* are interconnected by strong covalent bonds to form a chain becoming polyethylene (*PE*) and polytetrafluoroethylene (*PTFE*) [21, 22].

The molar mass of *macromolecules* may reach 10^3 or even 10^9 g/mol. The molecular mass of a polymer results from the degree of polymerization (*DP*) that represents the average number of *monomers* in a chain. In fact, each polymer has a lot of chains which are arranged in four possible ways corresponding to possible molecular structures of polymers. These structures, shown in Fig. 1.7, are generally called [21]:

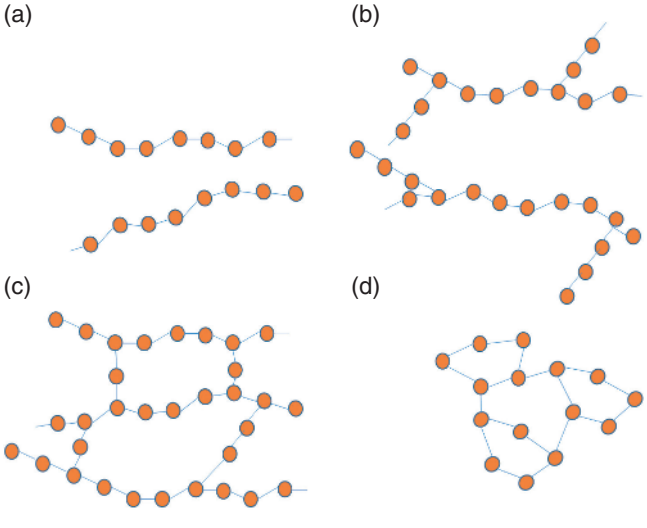

Figure 1.7 Possible molecular structure of polymers: (a) linear; (b) branched; (c) cross-linked; and (d) network or strongly cross-linked.

- ***Linear polymers,*** probably the most frequently used polymers, include the covalent bonded monomers in the chains, which are weakly bonded with other chains. The bonding between the chains is of hydrogen or *van der Waals type*. Examples of linear polymers *PE* are polystyrene (*PS*), poly (methyl methacrylate, *PMMA*), or high-density polyethylene (*HDPE*).
- ***Branched polymers*** include side branches lowering their density as in low-density polyethylene (*LDPE*).
- ***Cross-linked polymers*** have chains with additive molecules that are covalently bonded as in the rubbers.
- ***Network polymers*** or strongly cross-linked ones, which are composed of 3D covalently bonded monomers to which epoxy resin or polyurethane (*PU*) belong.

The classification of the polymers being most popular is related to their behavior in higher temperatures and under mechanical stress. Consequently, ***thermoplastics*** soften and deform easily in higher temperatures. The molecular structure of this type of polymers is linear or branched, and this group of polymers can be amorphous or crystalline (up to 90% of crystallinity). The opposite group of polymers is ***thermosets*** that do not soften with increasing temperature. *Thermosets* can have strongly cross-linked structures as epoxy resins. *Thermosets* with slightly cross-linked structure are called also ***elastomers***. Finally, there are also ***natural polymers*** such as [22]: (i) cellulose, which is main component of wood, cotton, and paper; (ii) keratin, present in wool fiber; and (iii) natural rubber.

The molecular structure of polymers determines their behavior in higher temperatures. The chains of molecules in *thermoplastics* and *elastomers* can easily move and change their position inside the body. Their specific volume[2] may considerably increase starting from the temperature called *glass transition*, T_g. The polymers have also melting point, T_m, but they do not have evaporation point, T_{ev}, as above the melting point, these materials decompose [22, 23].

The general properties of polymers can be synthesized after Seidel and Hahn [24]:

- density is in the range of $\rho = 0.8–2.2\,g/cm^3$;
- electrical resistivity is high leading to the frequent application of these materials as isolators in electric and electronic industry;
- high *TEC* being greater than in metals;
- high resistance against corrosion (depending on the type of polymers);
- rapid aging under external influence (*uv* radiation, thermal shocks, etc.).

The mechanical properties of polymers and, in particular, their stress vs. strain behavior depend on the type of polymers as seen in Fig. 1.8. The curve corresponding to *thermoplastics* (Fig. 1.8b) is similar to that of metals and alloys, and shows elastic behavior followed by plastic deformation.

The slope of the curve, i.e. Young modulus, E, for these materials depends however strongly on temperature and on the time of measurement. *Thermosets* (Fig. 1.8a) are harder and brittle without plastic deformation. Finally, *elastomers* (Fig. 1.8c) show only elastic deformation under very low stress.

2 Specific volume is inverse of density, i.e. $1/\rho$

The polymers used as substrates in films and coatings deposition are mainly *thermoplastics* and *thermosets*. Some properties of the most popular polymers are presented in Table 1.6.

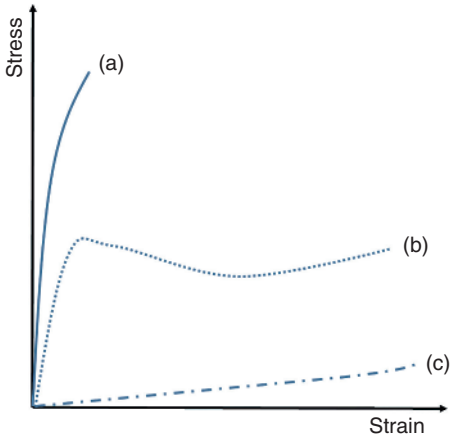

Figure 1.8 Typical strain–stress behavior of: (a) *thermosets*; (b) partly crystalline *thermoplastics*; and (c) *elastomers*. *Source:* Adapted from Callister [8].

Table 1.6 Some properties of frequently used polymers.

Type	Polymer	Glass transition temperature, T_g, K	Melting temperature, T_m, K	Density, ρ, kg/m^3	Modulus of elasticity at *RT*, *E*, GPa	References
Thermoplastics	Low-density polyethylene, *LDPE*	163	388	0.91–0.94	0.17–0.28	[8, 21, 23]
	High-density polyethylene, *HDPE*	183	410	0.95–0.97	1.08	
	Polyvinyl chloride, *PVC*	378	414	1.4	2.41–4.14	
	Polyamide, *PA6*	323	493	1.3	1.59–3.79	[21, 23, 25]
	Polycarbonate, *PC*	423	—	1.2	2.38	[21, 25]
Thermosets	Epoxy resin	380		1.2–1.4	2.1–5.5	[13]
	Phenol formaldehyde resin	—	—	1.27	8	
Natural polymer (wood)	Ebony	—	—	1.01	17.7	[23]
	Oak European	—	—	0.69	10.1	

1.3 Cleaning of Surface

The surface being prepared prior to a film or coating deposition has always some contaminants. These contaminants are hard to remove entirely but have to be reduced by cleaning to an acceptable level [26, 27]. The surface contaminations may result from:

- reaction with the environment (oxides, corrosion products, etc.);
- physical adsorption of the environment (water);
- traces of previous processes (polymer masks, oils, fingerprints, etc.);
- dust particles;
- degassing products generated during high-temperature action on the substrate (water, plasticizers, etc.).

The synthetic and naturals polymers are the class of materials used more and more frequently as the substrates for films, and interested readers may deepen the knowledge of chemistry and possible degradation of polymers in many references, such as [26].

The type of contaminants depend, to a degree, on the substrate material. Consequently, the surfaces of metal substrates are often covered with lubricating oils to protect them from corrosion during transport and storage. Ceramic substrates are frequently porous and can contain some water, which condensed from the vapors in the pores connected with the surface (called frequently *open pores*). Similarly, polymer substrates can also contain water and plasticizer added frequently to modify polymers' flexibility. Finally, all types of substrates can have dust or fingerprints on their surface.

The cleaning procedure depends also on the following film or coating deposition technique. Thin films obtained by atomistic methods need to be deposited onto surfaces and cleaned more carefully (having lower level of contaminants) than the coatings obtained by granular or bulk methods.

The cleaning methods are frequently composed of numerous steps. These steps can be roughly categorized as chemical and physical. An example of the TiNi-alloy surface preparation steps prior to Ti-film deposition by sputtering presented by Sonoda et al. [28] includes:

- polishing with emery paper;
- polishing with diamond paste and oil;
- washing with water and drying;
- ultrasonic cleaning with acetone.

It should be also stressed up that surface cleaning may be associated with the surface activation that is polishing with emery paper and diamond paste. In this chapter, the activation and chemical and physical methods cleaning are discussed separately.

1.3.1 Chemical Cleaning Methods

The chemical cleaning can be realized by [27, 29]:

- chemical etching, to be applied to remove some of the substrate making easier the removal of all type of contaminants;
- alkaline cleaning, converting organic fats into soaps easy to dissolve in water;

- chelating cleaning, to be applied for the phosphate contaminants;
- solvents cleaning, to be used to remove hydrocarbons as well as biofilm or protein contaminants;
- oxidation cleaning, to be used when oxides are volatile and is realized frequently using plasma discussed later in the section describing physical cleaning.

The chemical etching of metals and ceramics including composites as WC-Co is typically carried out using acids or bases. Table 1.7 shows some examples of chemical cleaning applied to treat different types of substrates. Polymer substrates have to be cleaned up with a detergent. Chemical cleaning can be also done with solvents. Polar contaminants should be cleaned up with water (used in solution with acids as shown in lines 2, 4, and 5 of Table 1.7), while non-polar contaminants, such as hydrocarbons, are to be cleaned with such solvents as ethanol, methanol, or trichloroethylene (see line 6 of Table 1.7).

Table 1.7 Examples of chemical cleaning.

No	Chemical cleaning using	Substrate	Film to be deposited	Deposition technique	Remarks	Reference
1	NaOH followed by HNO_3 or HNO_3/HF	Aluminum alloy	—		Second step is used to remove the residue of copper or silicon on the surface	[27]
2	Murakami solution: K_3 [Fe $(CN)_6$]: KOH: H_2O = 1: 1: 10	WC composite + 6 wt. % Co	*DLC*	*CVD*	Increase in Co/W ratio and of the roughness	[30]
3	NaOH and KOH heated solution				Removal of oxide product generated at plasma treatment	[31]
4	Solution of 2 vol. % HF in water, followed by rinsing in distilled water and washing with acetone	Si			Cleaning was followed by deposition of a bond-coat	[32]
5	$NH_4OH/H_20_2/H_20$ (1:1:5) at 348 K followed by rinsing in deionized water and by $HCl/H_2O_2/H_20$ (1:1:6) at 348 K	Glass	Thin-film transistors	—	Preparation for liquid crystal displays	[33]
6	C_3H_6O (acetone) followed by blowing with N_2 and CH_3OH (methanol)		Ti	Magnetron sputtering	Preparation to laser-assisted micro-joining	[34]

The removal of proteins is more complicated. It was tested for the substrates used as biomaterials in medical applications such as Ti (99.3 wt. % pure), Au (86 wt. % pure), dental ceramics[3], and polymers as *PMMA* and *PTFE* with different solvents by Kratz et al. [29]. The authors made up to 50 rinsing cycles. They found out that the solvent known under tradename of *RIPA* Buffer was composed of[4]: $NH_2C(CH_2OH)_3 \cdot HCl$ (known as *Tris* HCL) + NaCl + nonyl phenenoxypolyethoxylethanol (known as NP-40) + $CH_3(CH_2)_{11}SO_4Na$ (known as *SDS* or sodium dodecyl sulfate) was the best one compared to, e.g. ultrapure water, isopropanol, or only *SDS*.

Between the chemical cleaning steps, the substrate should be rinsed. The popular method is rinsing with deionized water. This water can be used a couple of times until the rinsing water reaches the prescribed electrical resistivity which gets lower with the dissolved impurities. Couillard et al. [33] started rinsing glass substrates with deionized water having resistivity greater than $\rho > 17\,M\Omega.cm$ and finished when this resistivity reached $\rho = 8\,M\Omega.cm$.

1.3.2 Physical Cleaning Methods

The physical cleaning leads to a removal of particles of different contaminants attached to the surface. The adhesion force depends on the surface's roughness and on the size and shape of the particles. The adhesive forces include after Cooper et al. [35]: (i) intermolecular *van der Waals forces*; (ii) various chemical bonds; and (iii) forces resulting from phenomena related to sintering such as diffusion. The authors determined experimentally and numerically the removal force of alumina particles having diameter of $d = 3.6\,\mu m$ to SiO_2 substrate having asperities up to about 2 nm to be about $F \approx 600\,nN$.

The physical cleaning methods are categorized in this section as: (i) thermal cleaning; (ii) particles cleaning which uses coarse (sand) and fine (atoms or ions) particles; and (iii) photons cleaning. The methods can be used in all films and coatings deposition methods depending on their specification resulting from the application.

1.3.2.1 Thermal Cleaning

Thermal cleaning is useful to evaporate such contaminants as water or hydrocarbons attached to metallic or ceramic substrates. Such cleaning may be associated with some negative effects such as: (i) diffusion of the contaminants in the substrate's interior; or (ii) oxidation of the substrate. To avoid these effects the heating can be applied after preliminary cleaning and in an inert atmosphere or under vacuum [27]. The heating may be realized in the conventional furnaces by convection or radiation and by using electromagnetic radiation at radio or microwave frequencies depending on substrate material.

The induction heating uses *RF* and can be applied for electrically conducting substrates. The heat is generated by *eddy currents*. Such heating can be generated very rapidly. Microwave heating can be applied for poor electrical conductors. The *dielectric heating* results from coupling of electromagnetic radiation with the dipoles in the substrate.

---

3 Product of VITA Zahnfabrik, Bad Säckingen Germany,
4 Proposed by, e.g. Merck, Darmstadt, Germany

1.3.2.2 Particles Cleaning

The particulate cleaning describes cleaning using small and large particles. Small particles such as ions, atoms, or molecules, which are used in cleaning by: (i) plasma; (ii) *i-beam* direct or being a part of sputtering; (iii) arc; and (iv) ultrasounds. The large particles, used for polishing, are in emery paper or diamond paste.

1.3.2.3 Plasma Cleaning

Plasma bombardment can be used with different types of plasma generators described by Thornton and Green [36]. This method is particularly effective *in situ* short before the deposition process. The *ex situ* method is often applied to clean up the surfaces of organic substrates. Cleaning with plasma is more efficient if the substrate is under negative potential to attract heavy positive ions. The electrically conductive substrates can compensate the arrival of such ion by a free electron and preserve a negative potential during all processing time. The dielectrics (oxides, polymers) do not have free electrons and would be charged with the positive ions and gradually repel them. This is why, the alternating current discharges should be used to generate plasma used to treat these types of materials. Moreover, the plasma for cleaning is typically generated with the use of an inert gas. The use of reactive gas to generate plasma may lead to plasma etching.

The plasma applied for cleaning is generated under low pressure being in the range of $p = 10^{-4}$ – 10 hPa. A few electrons (generated by field emission or ***photo – dissociation***) initiate their formation. The electrons are accelerated in the electric field and collide with atoms and molecules. If their energy is high enough ($E_e = 1$–10 eV, see Table 2.8), collisions are inelastic and result in the ionization or dissociation of working gases. The electrons formed in the collisions are generated in cascade and fill the volume of gas by creating plasma. The plasma remains in equilibrium if the number of electrons generated is equal to the number of electrons lost by recombination with positive ions or with neutral species capable of forming negative ions. The plasma is electrically neutral on the macroscopic scale. In contrast, microscopically, there are significant variations in potential. The electric field of each charged species is compensated by another charged species. The compensation distance is called the ***Debye radius***. The temperature of the electrons in low-pressure plasmas is 10–100 times higher than the temperature of the ions (see Fig. 2.17).

The plasma is generated by electrical discharges. Cleaning is typically done with plasma generated by:

- *DC* discharge;
- *RF* discharge;
- microwave discharge;
- ***post-discharge***, that is, plasma downstream of a discharge.

The discharges of different types are shown schematically in Fig. 1.9.

Discharge in a *DC* diode system (Fig. 1.9a) begins with an electrical breakdown in the gas. The breakdown voltage depends on the gas and its pressure. The space between the electrodes becomes a conductive plasma being close to the potential of the anode. The voltage drops near the cathode. The main source of electrons maintaining the discharge is ion bombardment of the cathode (substrate). This bombardment results in the emission of secondary electrons. If the ions have low energy, secondary electrons are emitted by the

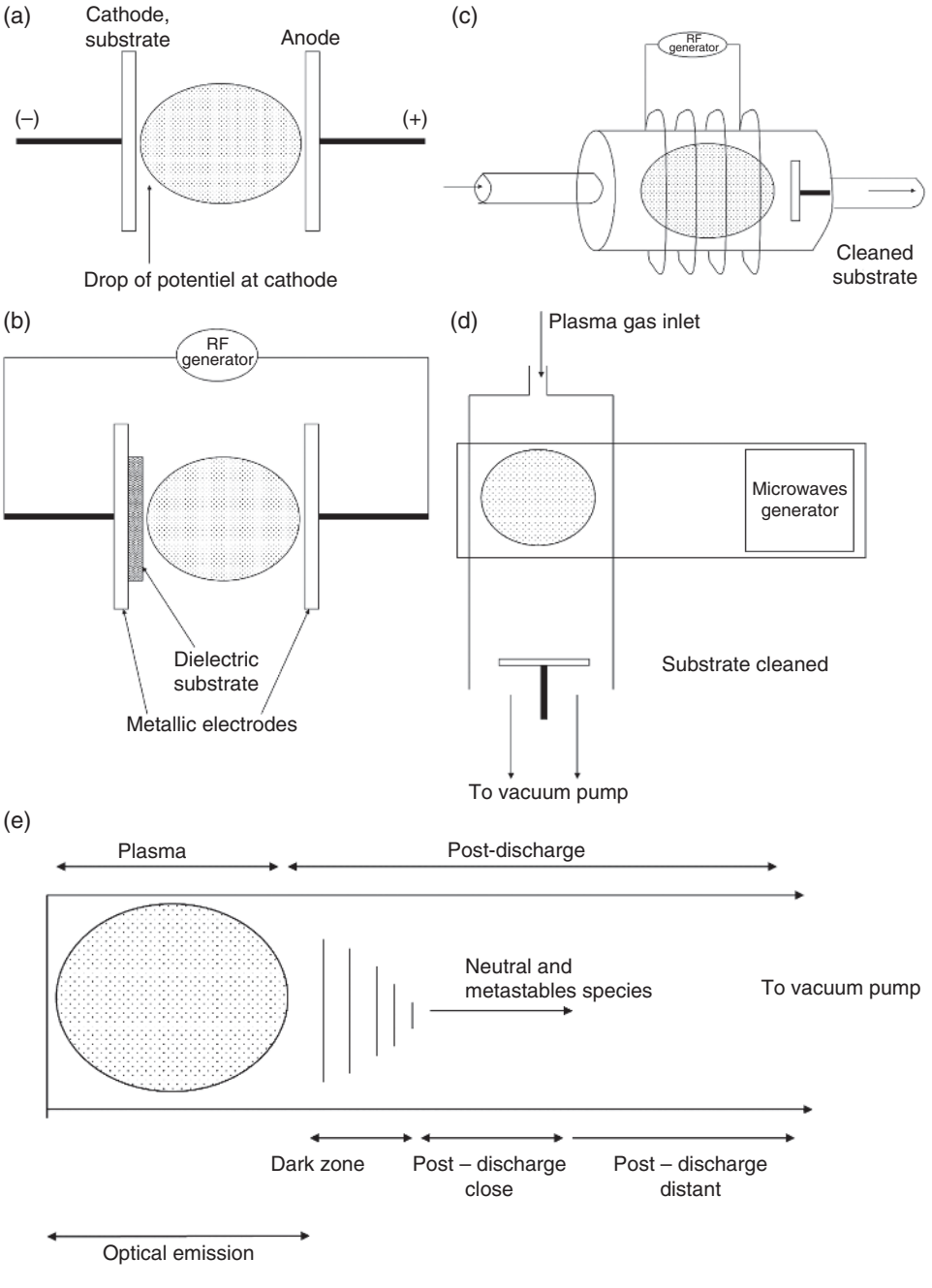

Figure 1.9 Types of plasmas generated by electrical discharges applied for cleaning or for etching surfaces of substrates: (a) *DC* diode discharge, (b) *AC* diode discharge, (c) *RF* discharge (*ICP*), (d) microwave discharge with a cleaned substrate downstream (in post-discharge), (e) characteristic areas of *post-discharge*.

Auger[5] mechanism, while the kinetic collision mechanism prevails for energy ions greater than 100 eV. The conductive substrate being put on the cathode potential is cleaned or etched by ion bombardment. The *DC* diode cleaning has the following advantages:

- plasma is uniformly distributed over large areas;
- system is simple;
- high-power densities are possible to reach.

A specific possibility of cleaning the oxides attached to a metallic substrate by an electric arc offers the technique of vacuum plasma spraying (*VPS*) belonging to the granular deposition techniques. This technique is sometimes used to spray superalloy coatings on turbine blades. After cleaning, the substrate is put on the negative potential and becomes a cathode, while the oxides contamination is the privileged place of attachment of electric arc. The arc heats up, melts, and removes the oxides.

Many problems are associated with the cleaning of dielectric substrates. The diode system, powered by alternating current at radio frequency, can be applied to clean such substrates (Fig. 1.9b). The diode system works usually at the frequency of $\nu = 13.56\,\text{MHz}$ and a peak-to-peak voltage greater than 1000 V [27]. The plasma is generated in this system by a capacitive coupling. The use of this system for conducting substrates would result in ion bombardment for half a cycle when the cathode is on negative potential, and the second electrode is bombarded during another half-cycle. Consequently, the substrate and the walls of an enclosure should be protected to prevent deposition of anode vapors. If the substrate is a dielectric plate fixed on a metal one, the system to be cleaned is then a capacitor with metal plate and plasma being conductors. The dielectric surface to be cleaned is periodically on a low positive potential and on a high negative potential because of inertia of the ions.[6] Cleaning by ion bombardment takes place when the surface of the dielectric is negative. *RF* plasma cleaning with capacitive coupling has the following drawbacks:

- *RF* energy losses in the system;
- lack of uniformity of the plasma on surfaces with complex geometry.

The inductively coupled plasma (*ICP*) system, shown in Fig. 1.9c, also works with the frequency of $\nu = 13.56\,\text{MHz}$. Its advantage is the lack of contact between the plasma and the electrodes. The gas is not contaminated and is therefore more useful to be used for plasma cleaning and etching the substrate.

The microwave discharge (Fig. 1.9d) uses frequencies from $\nu = 300\,\text{MHz}$ to 10 GHz. Microwave plasma is characterized by the higher degree of ionization compared to the plasmas described above. This plasma is often applied to clean or etch the substrates in the *post-discharge* configuration shown in Fig. 1.9e. Such treatment is recommended when

5 The mechanism of the excitation of an atom by an emission of electrons whose energy is weaker than the energy of incident ion. The emission of an Auger electron is associated by a photonic emission or another forms of an excitation

6 Ions are too inert to follow the electric field at a frequency greater than 100 kHz. Consequently, one electrode being initially more positive with respect to the earth potential collects electrons quickly, while the other electrode collects ions less quickly [37]. Finally, an electrode acquires a permanent negative potential and becomes a privileged target of ion bombardment.

there is a possibility that the surface of a substrate may be damaged by highly energetic species. These species are still present in the neighboring plasma area (***dark zone*** in Fig. 1.9e). However, their density decreases rapidly due to ***ambipolar diffusion***[7] and to the recombination of species on the walls of a reactor. Consequently, the emission of photons is less intense in this area than in the plasma. The next area downstream of the plasma is called the ***close post-discharge*** zone. It is characterized by the presence of excited molecules and of long-lived radicals. There are almost no ions, and the optical radiation is very weak. In the last ***distant post-discharge*** zone, there are only long-lived metastable species and free radicals. Mézerette et al. [38] reported that carbon contaminants are removed from an iron foil cleaned by Ar-N_2 microwave post-discharge at frequency of $\nu = 2.45\,\text{GHz}$ as CN^* radicals. In order to avoid nitrogen grafting to the substrate, the authors recommended heating up of substrate at post-discharge cleaning to $T = 373\,\text{K}$.

Other types of plasma applied to cleaning are, among others: (i) plasmas generated by electronic emission (e.g. by a hot wire); and (ii) plasmas confined in the magnetic field. These plasmas are generated in the installation for films deposition by *CVD* and *PVD* and are described in chapter 2.

1.3.2.4 Ions and Atoms Bombardment

As described above different types of plasma clean the substrates by heavy species bombardment. The bombardment may have many effects. These effects depend on plasma and on substrate and in particular on:

- mass, flow, and energy of bombarding species;
- nature and mass of the atoms of the substrate;
- nature and mass of the contamination atoms.

During the cleaning process only the first of these elements can be controlled. The energetic species interact during the bombardment with the ones being present on the surface (contamination, atoms of the substrate), and this interaction can result in the following effects [39]:

- desorption of contaminating species and setting them in motion;
- implantation of contaminating species in the substrate;
- creation of a structural defect caused by a cascade of collisions with the atoms of the substrate;
- implantation of a bombarding species in the atomic lattice of the substrate or in its structural defects;
- chemical reactions of the species present at processing;
- sputtering of the species present on the substrate's surface by the cascade of collisions which can be followed by back-scattering and their return back and re-deposition on the substrate;

  i.e.
- emission of secondary electrons;
- rebound of energetic species;

7 A movement of ions in one direction and electrons in the opposite direction

- transfer of the effects of the bombardment inside the substrate by the effect of a ***channeling***;
- heating of the substrate.

Among these effects, the most advantageous for cleaning are: (i) desorption of contaminating species; (ii) sputtering of the species present on the substrate's surface; and (iii) chemical reaction. These effects will be discussed in detail.

The choice of operational cleaning parameters should favor these effects. Desorption of contaminating species is desired because it leaves the surface clean of those species that are weakly attached to the surface by *van der Waals forces*. Contamination, which is better attached to the substrate's surface, can only be removed by sputtering.

Sputtering is, in fact, an effect used for one of the *PVD* deposition processes. The *PVD* deposition is done by using ions having energies sufficient to detach the atoms of a target and to move them toward a substrate to form a film. The cleaning and etching is made with the ions having energy ranging from 30 eV to 3 keV [40]. Consequently, Ochs et al. [41] used ions generated in the gases Ar, O_2, and Ar/O_2 having energy up to $E_i = 0.35$ keV to clean up the glass substrates by removal of carbon-containing contaminants. To generate them one can apply the plasma at high pressure or a post-discharge plasma with a weak polarization of the substrate. The application of ion -beams under low pressure enables avoiding the back-scattering and re-deposition discussed above. The *i*-beam can be directed under incident angle different to 0° (normal to the surface). To take an example, Goto et al. [42] used angle of 10–55° to clean up the ceramic substrate prior to the deposition of *YBCO* high-temperature superconductor film.

The chemical reaction with the plasma species does not depend very much on the energy of the ions bombarding the surface, which can remain very weak, but mainly on the chemical composition of the plasma. To clean the surface, it is preferable that the products of reaction are volatile. The process of surface cleaning by chemical reaction is called plasma etching and has been applied since the 1970s – in the electronics industry to treat semiconductor materials. The plasma gases used for plasma etching are typically chlorides or fluorides (Table 1.8).

Table 1.8 Substrates materials etched by different low-pressure plasmas.

Substrate	Plasma gas
Si	Cl_2, CCl_4, CF_4, NF_3, SF_6
SiO_2	CF_4/H_2, CHF_3, C_2F_6
Si_3N_4	CF_3Br, CF_4
WSi_2, $TaSi_2$	CF_4
Al	BCl_3, CCl_4, Cl_2
Ti, Mo	CF_4
Au	Cl_2
GaAs	Br_2, CCl_2F_2, Cl_2, CCl_4
InP	Cl_2, CCl_2F_2, CCl_4

Source: Curran [43]/IOP Publishing.

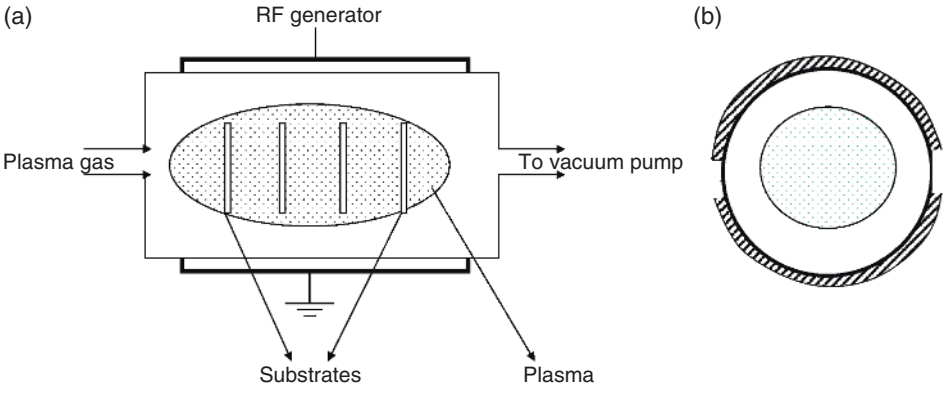

Figure 1.10 Reactor with capacitive coupling having cylindrical electrodes (*barrel etcher*): (a) longitudinal section including substrates; and (b) cross-section of the reactor.

The plasma etching is often carried out using RF plasma in cylindrical reactors using inductive (Fig. 1.9c) or capacitive coupling in a configuration with flat (Fig. 1.9b) or cylindrical electrodes as in ***barrel etcher*** shown in Fig. 1.10a,b. An example of plasma etching using such installation was GaAs substrate treated with plasma generated using the gas mixture of CCl_2F_2 and Ar. The etching rated was about 200 nm/min [43]. This process can be applied for removal of organic contaminants for example the remaining organic masks (photoresist) used in ***photolithography*** or oxidation of polymers with oxygen plasma.

1.3.2.5 Ultrasonic Cleaning

Ultrasonic cleaning uses ultrasounds having frequency $\nu = 20$–40 kHz to agitate a liquid. The fluid is generally water, which can be used for ceramic or glass substrates, but other solvents can be used to clean metals and alloys. The process uses cavitation bubbles induced by the waves generated by ultrasound. The cleaning process is relatively short (few minutes), and the cleaning of blind holes in a substrate is possible. However, the action of the bubbles collapsing on a surface may lead to its erosion and fracturing [27]. To show an example, Jundale et al. [44] cleaned ultrasonically the amorphous glass substrates prior to the deposition of $CoFe_2O_4$ films by spray pyrolysis.

1.3.2.6 Photons Cleaning

The cleaning with the photons is realized nowadays mainly using lasers. The lasers used in industry are shown in Table 1.9. They emit radiation of different wavelengths, starting from *uv* (excimer laser) up to far *ir* (CO_2 lasers). The laser beam is focused on the surface of cleaned material. A part of laser power is reflected from the surface, while another part is absorbed. The reflectivity, R, and the depth of absorption, L, for some materials are shown in Table 1.10. It is possible to see that the major part of radiation at far *ir* ($\lambda \approx 10\,\mu$m) is well reflected by metals. The metals and alloys are to be treated rather by Nd: YAG laser. Consequently, the radiation of CO_2 laser matches better to treat ceramics. The optical properties result from the electronic structure of ceramics, which have completely filled valence bands, and no free electrons are available and the radiation is absorbed by the high-frequency

Table 1.9 Industrial lasers used in surface cleaning [15, 45, 46].

Parameters	CO_2 – laser	Nd: YAG – laser	Excimer laser	Diode laser	Fiber laser
Wavelength range, μm	10.6	1.06	0.2–0.3	0.4–3.3 depending on emitting diode	0.9–1.55
Continuous – C/ pulsed – P	C/P	P/C	P	P/C	P/C
Maximal average power, kW	25	2	0.4	4	20
Beam quality	Very high	Low	Low	High	Excellent

Table 1.10 Optical data for selected metals and oxides at the wavelengths about 1 and 10 μm.

Material of substrate	Wavelength, λ, μm	Reflectivity, R, dimensionless	Optical absorption depth, L, μm
Al	9.54	0.99	0.21
	0.83	0.87	0.022
Ni	9.54	0.98	0.14
	1.03	0.72	0.046
W	10	0.98	0.16
	1	0.58	0.068
SiO_2	10.6	0.2	40
	1.06	0.04	>106

Source: Pawłowski [47]/Springer Nature.

phonons. The detailed information concerning the interaction of lasers with different materials is presented in the chapter describing laser methods of films and coatings deposition.

The properties of the surfaces to be cleaned can be modified by covering them with a film of water. The water film evaporates explosively when intensively heated by laser [46]. The vapors expels the particles of contaminants. Contrary to such ***wet cleaning***, the ***dry cleaning*** by laser, working in pulsed mode, is associated generally with a laminar inert gas flow parallel to the surface which removes the detached particles. The contaminants particles may be detached by the following way [46, 48]:

- ***Laser-induced surface vibration***, which results from cyclic thermal expansion of substrate during incoming laser pulses. The heating and cooling cycles result in vibrations of cleaned surface transferred to the contaminating particles, which are ejected.
- ***Particle vibration*** results from direct absorption of laser energy by particles. The laser pulses induce a light pressure on the particles leading to their possible ejection from the cleaned surface.

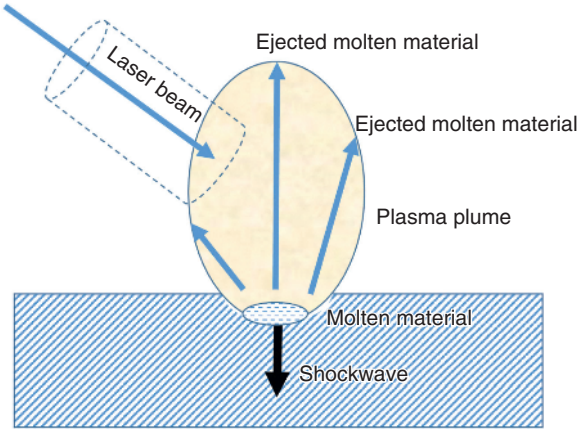

Figure 1.11 Sketch of laser ablation.

- ***Particle thermal expansion*** is induced by heating and cooling by laser pulses. The cyclic modification of particles size may lead to their detachment followed by ejection.
- ***Ablation***, shown schematically in Fig. 1.11, consist of formation of plasma plume by a laser pulse. The plume absorbs incoming energy and interacts with the cleaned surface by action of thermal shocks and rapid heating associated with evaporation of contaminants. Nd: YAG and excimer pulsed lasers are particularly well adapted to clean up by ablation the metallic substrates.

An important practical issue is time of cleaning. A choice of laser and its wavelength, the mode of action (continuous or pulsed), its density of energy or power are made in function of contaminant and of cleaned material (see Table 1.11). The surface is cleaned by the scans of a laser beam, and the velocity of the scanning is an important parameter to be optimized. It determines the time of treatment, which may be long especially for large surfaces to be treated. Laser cleaning is useful in many industrial applications, such as aeronautic, building, and maritime industries, as shown in Table 1.11. Razaba et al. [54] reviewed laser cleaning in automobile industry. Reitz [46] described laser cleaning of electronic components and artworks.

1.3.3 Monitoring of Surface

Monitoring can be roughly divided into two categories: (i) development of cleaning procedure; and (ii) routine monitoring of surfaces before films and coating deposition. The test at the development of the procedure includes mainly the microscopic observation of cleaned surfaces topography with the use of optical and scanning electron microscopes (*SEM*). Details having size in a nanometer range or even smaller can be observed with atomic force microscope (*AFM*). The surface chemistry, i.e. identification of elements, can be tested using X-rays photoelectron spectroscopy (*XPS*) or X-ray fluorescence (*XRF*). Finally, the crystal phases present on a surface can be identified using X-ray diffraction (*XRD*). All these methods are used also to characterize films and coatings, and are described in the chapter dealing with their characterization. The surface cleaning specifications may include other properties, such as hydrophobicity. In this case, it is useful to carry out the

Table 1.11 Examples of laser cleaning for different application.

Laser type → / Cleaning details ↓	CO_2	Nd: YAG	Excimer	Diode	Fiber
Wavelength, λ, μm	10.6	1.064	0.248	0.81	1.064
Mode pulsed/ continuous (P/C)	C	P	P	C	P
Laser power, kW	0.13	0.1–88	—	0.06	0.2–0.8
Pulses parameters		$\tau = 100$ ns, $\nu = 1$–30 kHz	$\tau = 25$ ns, $\nu = 4$ Hz, $E = 650$ mJ		$\tau = 30$ ns, $\nu = 20$ kHz
Scan speed, mm/s	25	50	—	250	4000
Substrate	Ti alloy		Ag	Concrete	Al alloy
Contaminants	Oil film		Sulphur	Chlorinated rubber	Marine biofouling film
Industrial field of application	Aeronautic		—	Building	Maritime
Remarks	Ar with O_2 atmosphere	—	Laser KrF, fluence 200–400 mJ/cm^2	O_2, N_2, or Ar atmosphere	—
Reference	[49]	[50]	[51]	[52]	[53]

measurement of wetting angle. Tian et al. [53] made such measurements for different fiber laser fluencies by cleaning of biofouling from aluminum alloy surfaces. The authors found out that laser cleaning with the greatest fluency results in greatest wetting angle indicating surfaces with excellent hydrophobicity.

Mattox [27] proposed a couple of simple quality tests for glass surface cleaning. The *water-breaking test* consists of observations of water sheet, which breaks up on the surface impurities and remains continuous on the clean surface. Even simpler is a *water condensation test*, which shows the impurities of the surface covered with thin condensed water vapors. This test can be done each morning on the mirror of the bathroom after a shower.

1.4 Patterning of Films and Coatings

The films and coatings are frequently designed to have a particular shape, which results from the function to be fulfilled. The patterning is particularly often used in atomistic films. The desired planar shape of a film can be reached by different types of ***lithography***, which consists of masking the area where this film should not be deposited. An alternative technology is ***direct patterning*** which consists of deposition of the film in desired area on a

substrate. Finally, the *mechanical* or *stencil masks* are used in thermal spray technology which is an example of particular coatings deposition. The patterning using ***mechanical masks*** is easier and cheaper than post-deposition grinding of coating. Such masking can be made using, e.g. temperature-resistant tapes, steel, aluminum foil, and wires. Dupuis et al. [55] applied such patterning to the manufacturing of a pyramidal array with the use of cold-spray technology.

An important issue is the size of the planar objects to be reached by patterning. This size decreases rapidly; the driving force behind this tendency comes from electronic and semiconductor industries manufacturing the integrated circuits (*IC*) using planar technologies on silicon substrates (so called *wafers*). The integration of these circuits increases steadily to reach a very large scale of integration (*VLSI*), and the size of planar elements composing a circuit stepped down to reach at present 10 nm [56]. The empirical ***Moore law***, valid in semiconductor industry since the beginning of 1970, predicts that the number of transistors in an *IC* grows exponentially (see Fig. 1.12).

Consequently, the patterning methods are different for preparation of micro-sized and nano-sized planar objects [57].

The *direct patterning* or *mask-less manufacturing* of planar objects can be made with use of different types of laser or with particles (electrons, ions) beams [2, 58]. In particular, laser patterning includes chemical transformation under action of photons. Finally, some granular techniques, such as cold spraying, enable the *direct patterning* of the planar objects of large sizes (cm). This technique is useful in a rapidly growing field of ***additive manufacturing***.

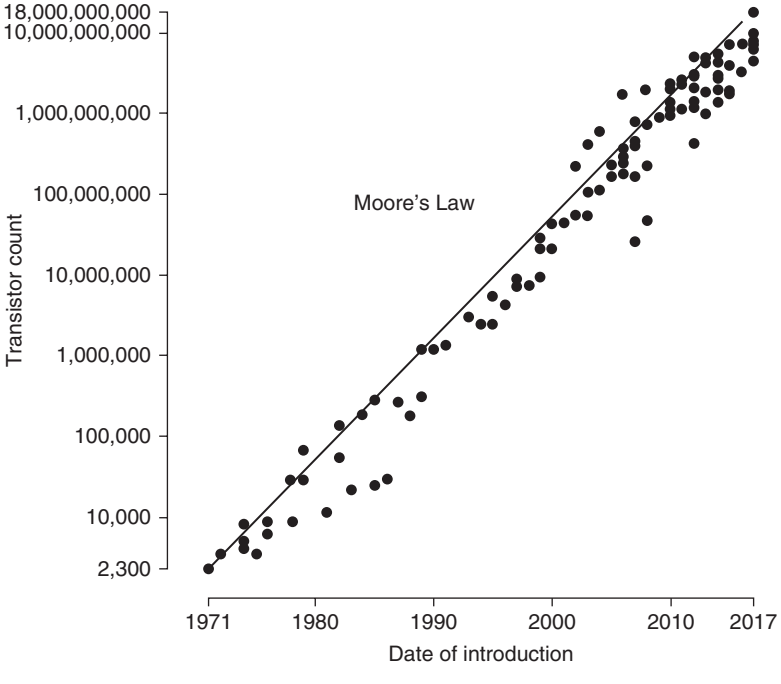

Figure 1.12 Illustration of empirical Moore's law valid in semiconductor industry [56]. *Source:* Reproduced with permission.

1.4.1 Lithography

Lithography means originally (ancient Greek) printing of an image drawn on a surface of stone on another smooth surface [59]. *Lithography* uses different ways of illumination such as: (i) *uv* light in *photolithography*; (ii) X-ray lithography; and (iii) particles (ions or electrons) beams lithography. The pattern is generated initially in a photo-mask, *PM* (to be used many times), and is shifted on a photo-resist, *PR*, being a *uv*-sensible polymer. The *PM* is made, typically, on a glass plate. The final pattern on a substrate is transferred by a development and removal by etching of *PR*. The sketch of photolithographic processes is shown in Fig. 1.13. The stages include:

- Cleaning of a substrate, which is followed, for *IC* preparation on a Si *wafer*, by oxidation to get a barrier layer and application of a photo-resist (*PR*) as seen in Fig. 1.13a. The *positive photo-resists* are easily soluble after *uv* illumination and negative ones are less soluble. Some authors recommend using bottom organic antireflective coating (*BARC*) to avoid the *uv* light reflection under *PR* and to improve its efficiency [60]. The *PR* is frequently applied by centrifugal spinning and baked (pre-baking).
- The *PM* is subsequently aligned above the *PR* (Fig. 1.13b). The mask can be in a direct contact (*contact printing*) or in a small distance of tenths of 15 μm to avoid contamination (*proximity printing*). Finally, the mask can be set at a distance of a few cm in so-called *projection printing*. The following step is the exposure to *uv* light illumination (Fig. 1.13c).
- The exposed part of positive *PR* is dissolved by a solution called frequently "developer" and removed from the substrate leaving the places on the substrate ready to be coated (Fig. 1.13d). The remaining *PR* should be hard-baked again to improve its resistance against deposited film. The etching process may be applied to clean up the part of the substrate to be deposited. The deposition of a film follows.
- The final stage of photolithography consists of removal of residual *PR* to leave a patterned film on the substrate (Fig. 1.13e). The removal can be made using oxygen-containing plasma, which oxidizes *PR* and detaches it from the substrate.

The processes are similar in all kinds of lithographic processes and will be analyzed more carefully in following sections. Some practical applications in different technologies of elements including films deposition will be also presented.

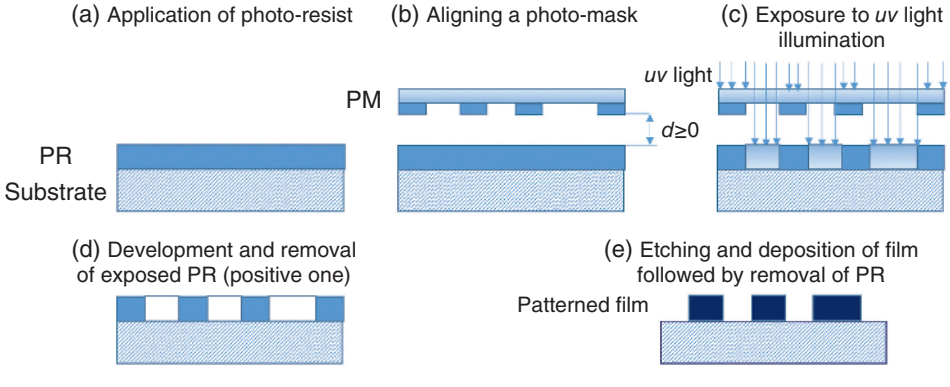

Figure 1.13 Sketch of patterning of a film with photolithography: (a) application of *PR*; (b) aligning of *PM*; (c) illumination with *uv* light; (d) development of *PR*; (e) removal of *PR*.

1.4.1.1 Illumination

Illumination is an important part of *photolithography* as well as *direct patterning*. It is realized using light or beams (X-ray, ions, or electrons). The description of *X-ray lithography* can be found elsewhere [59]. This section describes the particles' *e*- and *i*-beams. The simplified geometry of illumination at projection printing includes a lens and an aperture of a *PM* as shown in Fig. 1.14.

Light

An important parameter enabling obtaining a clear image of an aperture on the *PR* is resolution, which determines the minimum size of a pattern to be printed. The resolution[8] in the direction x or y, i.e. on the surface of *PR*, δ_x or δ_y, for light illumination is given, for the geometry shown in Fig. 1.14, in a medium having refraction index, n, by ***Abbe's equation*** [61]:

$$\delta_{x,y} = \frac{\lambda}{2n\sin(\theta)} \tag{1.7}$$

Knowing the value of refractory index for air $n = 1$, the value of product[9] $n\sin(\theta)$ can reach the value of 0.8 [62]. Consequently, it is possible to understand the reason of applying illumination with particularly short *uv*, being also called deep ultraviolet (*DUV*), such as emitted by excimer lasers having wavelength of $\lambda = 248\,\text{nm}$ or ArF with wavelength of $\lambda = 193\,\text{nm}$. Similarly, the Nd: YAG laser may have shorter wavelength than $\lambda = 1062\,\text{nm}$ by using the different harmonics of laser frequency, namely $\lambda = 532\,\text{nm}$ or even $\lambda = 266\,\text{nm}$ [58]. Lithography with the wavelength of $\lambda = 248\,\text{nm}$ together with small thickness of *PR* was used to obtain the elements of semiconductor devices smaller than 50 nm [60]. However, to obtain the nanostructural size objects shorter-wavelength illumination sources are

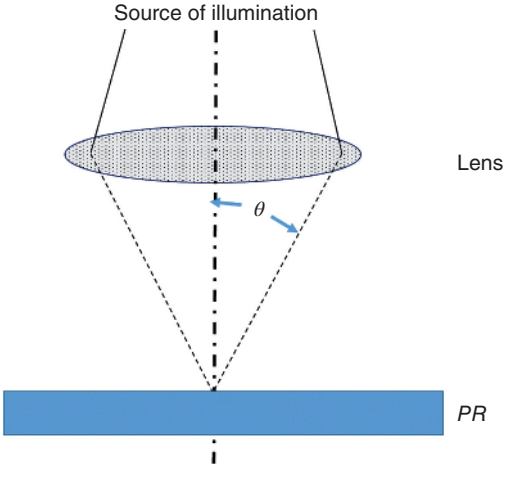

Figure 1.14 Simplified geometry of illumination at lithography.

8 The resolution has the same order of magnitude as, frequently used in the literature concerning lithography, critical dimension (*CD*) being a minimum size of a manufactured element

9 The product is also called numerical aperture, $NA = n\sin(\theta)$

recommended [57], such as *soft X-rays* having the wavelength of a few nanometers as well as particles beams described in the following section.

Particles Beams

Each particle can be associated with a wave following ***de Broglie hypothesis***. Its wavelength can be found by knowing particle's velocity and mass from the following equation:

$$\lambda = \frac{h}{m v} \tag{1.8}$$

The electrons and ions may be accelerated by electric field, and their wavelengths for different velocities are shown in Table 1.12. The application of the beams of electrically charged particles in lithographic process is however different from that of electrically neutral photons. The particles may interact with *PR* and induce some chemical and physical changes. Additionally, their penetration depths and profiles are different [57]. The *e-beam lithography* was used, e.g. for patterning of Mo/Si multilayer system to obtain structures having an accuracy of a few nanometers [63]. The *i-beam lithography* using heavy ions such as Ga^+ or of protons H^+ have an advantage, compared to *e*-beams, of greater penetration and giving straighter paths at patterning [59].

1.4.1.2 Masks

The masks used in lithographic processes can be made of different materials using different technologies as shown in Table 1.13.

The materials of masks include metals, ceramics, and polymers sometimes prepared as multi-films. The choice of materials is consistent with entire technology of planar objects manufacturing. The applications are mainly in microelectronic industry and the substrate is frequently silicon *wafer*. The patterning of the masks is realized by different methods including photolithography or "natural" patterning by the holes formed at growth of anodized alumina films. Finally, the geometry of films masking is discussed in the next section.

Table 1.12 Wavelengths corresponding to particles having different energies and velocities[a].

Particles	Velocities (km/s)	Kinetic energies, eV	Wavelengths
Electrons	100	0.0284	7.27 nm
	500	0.711	1.45 nm
	1000	2.84	0.727 nm
Protons, H^+	100	5.22	3.96 pm
	500	1300	0.793 pm
	1000	5220	0.396 pm

[a] Mass of an electron is $m_e \approx 9.11 \times 10^{-31}$ kg and mass of a proton is, $m_p \approx 1.67 \times 10^{-27}$ kg.

Table 1.13 Different masks used in lithographic processes of film patterning.

Mask material	Kind of patterning	Thickness, nm	Substrate	Geometry of film masking	Final application	Reference
Cr	Photolithography	4, 14, and 114	Si	Proximity printing	Capacitive microphone	[64]
Ni	*EBPVD*	15	Sapphire	Contact printing	Light-emitting diode	[65]
Al	Diamond tip of *AFM*		Si		Development of *AFM* lithography	[66]
PI/ Si/ *PMMA*	*e-beam* lithography	*PI* – 600, Si – 40, and *PMMA* – 200			Bragg-mirrors	[63]
Al_2O_3	Holes formed at anodizing	700	Al_2O_3		Nanodot arrays	[67]
SiN	—	500		Proximity printing	3D patterns	[68]
DLC	*ICP*	—	Si	—	Development of hard mask	[69]

1.4.1.3 Geometry of Lithography

The geometry of lithography depends mainly on the distance between the photo-resist (*PR*) and photo-mask (*PM*) during exposure to light or beams. The possible geometries, being also the ways of printing the form of the mask, are shown in Fig. 1.15. The methods include following ways of printing [59]: (i) contact; (ii) proximity; and (iii) projection.

The contact printing has an advantage of the highest possible resolution, but the mask gets used in contact with the *PR*. The damage of the mask is reduced at proximity and entirely eliminated at projection printing.

1.4.1.4 Etching and Removal Processes

Etching and removal occur many times during lithography. They are applied to the photo-resists (*PR*) exposed to illumination and are used to remove the residual one (see Fig. 1.13d, e).

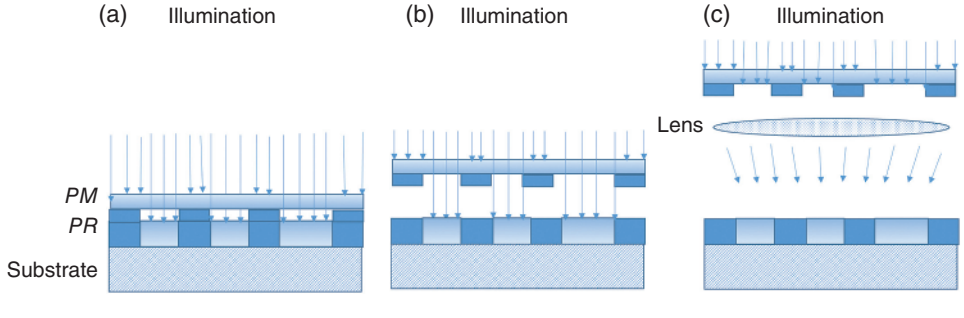

Figure 1.15 Possible geometries of *PM* and *PR* at following lithographic printing: (a) contact; (b) proximity; and (c) projection. *Source:* Adapted from Sebastian et al. [59].

Some planar technologies are realized with the *PM* being in direct contact with *PR* (see Fig. 1.15a). This requires also etching and removal of the masks and deposited films made of different materials. The etching can be roughly categorized as: (i) wet, realized with the liquids; and (ii) dry, done mainly using plasma gazes including reactive ions in a process called *reactive ion etching* (*RIE*).

Wet etching with the use of the alkaline aqueous solution (having $pH > 7$) is recommended for polymer *PR* after exposition to illumination [59]. Liu et al. [70] described a technology including etching of double-layer mask including Mo and SiO_2. The Mo layer was etched by a solution of HNO_3, H_3PO_4, CH_4COOH, and H_2O. SiO_2 was etched with a solution of HF, NH_4F with H_2O called buffered oxide etch *(BOE*).

Dry etching is frequently made using inductively coupled plasma (*ICP*) shown in Fig. 1.9c with an industrial frequency of $\nu = 13.56$ MHz. The *RIE* processing of a multilayer including Mo and Si was made with plasma gases including CF_4, SF_6, CHF_3, O_2, and Ar [63]. Nitride layers of GaN and InGaN were etched using plasma working gases Cl_2 with Ar [64]. Finally, the polymer *PM* was reportedly etched using O_2 with N_2 plasma working gases having optimized composition [60].

The final removal of polymer *PR* is also made using plasma containing O_2, which oxidizes it in a process called *plasma ashing* in semiconductors technology.

1.4.2 Direct Patterning

The very fine dimensions of photons or particles beams and the possibility of precise control of their movement by the robots controlled by computers enable the direct patterning. The process does not use masks and is called by some authors, such as Mayer and Allen [58], selected area processing (*SAP*). The patterning can be used to manufacture the unique products as well as many identical ones. The beams can be used to deposit directly the desired film or to create a pattern with a compound being as a gas or solid close to substrate's surface. The beams actions may have physical characters such as heating, scattering, or diffusion, or chemical ones such as photochemical synthesis or decomposition. These fundamental aspects are well described in the references [2, 58], and the sections below focus rather on the beams application.

1.4.2.1 Photons Patterning

The laser beams focused on a substrate may lead to local growth of films on the substrate by photon-activated reactions of the decomposition of gas- and solid-phase compounds and the reaction of oxidation. The gaseous compounds should be in the neighborhood of substrate surface, and the solid ones should be deposited on it. An example of reaction in gas phase is the decomposition of $(CH_3)_2Cd$ and subsequent nucleation and growth of Cd film on SiO_2 substrate [58]. The authors of [2] described solid-phase decomposition of $Cu(HCOO)_2$, at temperature of 620 K by action of the CO_2 laser working in continuous mode to form Cu film on SiO_2 substrate. Another possible reaction assisted by laser is local oxidation of Cr film deposited onto glass surface to form Cr_2O_3. This kind of patterning may be used to manufacture wear-resistant photo-masks.

Lasers may be also useful to etch the surface locally. The mechanisms of etching involve mainly [71]: (i) ablation; (ii) photo-chemical reactions in gas- and liquid phases;

and (iii) photo-thermal processes. The processes may occur simultaneously. For example, photo-thermal and photochemical processes enabled local etching and reduction of graphene oxide to graphene using a femtosecond laser having wavelength of 800 nm [72]. The examples of etching for all types of materials including metals, semiconductors, ceramics and polymers using different lasers are described in [2].

1.4.2.2 Particles Patterning

The *e*-beams have been used in mask-less patterning since 1970. The main advantage is high resolution of such patterning resulting from the wavelength associated with the particles being smaller than 10 nm as shown in Table 1.12. The patterning may be carried out on photo-resists such as *PMMA* or *Novolak* and is used frequently to fabricate the photo-masks. The process is however slower than *photolithography* [59]. The *i*-beams applied in ***mask-less lithography*** use light ions such as H^+ or heavy ones such as Ga^+. The interaction of heavy ions with the substrate surface may lead to the formation of defect sites. The sites are useful as nucleation centers on nonreactive surfaces [58]. These authors give the example of the beams applications. Consequently, the *e*-beam having energy of 3 keV was used for the nucleation of Fe film on Si by decomposition of gaseous-phase $Fe(CO)_5$ at temperature of 423 K. On the other hand, the Ga^+ beam having energy of 50 keV enabled growth of Fe and Al films on SiO_2 substrate. It is possible to use the heavy ions to get implanted as atoms in the substrate. The resolution of *i*-beams is very high, and the lines of GaAs having width of only 2–3 nm were manufactured with such beam [57].

1.5 Activation of Substrates Surface

The surface of a substrate is frequently activated to obtain or to improve the adhesion of films and coatings. The adhesion is related to the properties of the deposit and substrate, which determine the phenomenon occurring at their deposition and can be called ***intrinsic adhesion***. Other phenomena influencing adhesion occur during their service.

The *intrinsic adhesion* depends mainly on [73]:

- surface of the substrate including its roughness and *surface energy*;
- chemical affinity and, in particular, that of similarity of crystal lattices between a deposit and a substrate and on impurities sand structural defects in the film/coating;
- size, shape, and energy of the species building up the deposit resulting in the deposits microstructure;
- difference between the coefficients of thermal expansion, *TEC*, of the film/coating and the substrate in the case of a deposition process in the temperature much higher than the ambient one; and
- internal stresses in deposit and on their thickness.

The species forming film in atomistic methods of deposition are atoms and molecules. Their sizes are in the nanometers range, being much smaller than that used at granular deposition methods. The latter used the species having size in the range of tenths to hundreds of micrometers. Consequently, the adhesion mechanisms and the factors influencing

it are totally different. In atomistic methods, these factors are related to nucleation of the islands forming film and may concern the atomic defects of substrate or small impurities attached to them. The species used at granular deposition as thermal spraying are 10^3–10^4 greater and arrive being molten on the substrate surface. The adhesion of coating depends in this case on the substrate roughness and on their chemical affinity. The latter may enable the rapid diffusion of the atoms of the impacting particle to the substrate. The rapidity of the diffusion results from the short time of solidification of particle (in the range of microseconds) and of its cooling (seconds to minutes) [74]. The methods of surface activation are consequently very different and are discussed separately for atomistic and granular methods of films and coatings deposition. The process of bulk coatings generation is associated with melting of substrate's surface. Consequently, the surface preparation is less important than an interaction between solid reinforcement and liquid metal [75].

The ***adhesion in service*** is related to the phenomena occurring at films and coatings service. For example high temperature at service of coatings being part of thermal barriers or mechanical stresses occur in the films on the cutting tools, and may depend on the nature and level of thermal stresses (e.g. thermal shocks) and mechanical stresses. The mechanical properties, especially of elasticity modulus, E, of the coating and of the substrate play also an important role.

The difference of these two types of adhesion becomes evident when a film/coating adheres to the substrate after deposition procedure but detaches off the substrate at its service. Another example is a *DLC* film, which has excellent mechanical properties but cannot withstand the stresses generated at application on the surface of cutting tools.

Intrinsic adhesion can be improved by the various pre- and post-deposition treatments, while *adhesion in service* can also be improved by applying a bond-coat. The bond-coat for metallic substrates is typically a metal or an alloy, whose properties (*TEC*, E) are frequently intermediate between the substrate and the deposit.

1.5.1 Activation of Substrates at Atomistic Deposition

The atomistic deposits starts to grow by formation of clusters of atoms or molecules followed, generally, by formation of islands. This growth, described in detail in the appropriate chapter, depends on many parameters including substrate and its contact with growing films. The analysis of evaporated Al and Ti films nucleation and growth on different substrates did show that the stresses generated at the films' growth might modify the type of growth from island to layer-by-layer growth [76–78]. The stresses resulted from the presence of gases incorporated in the substrate.

Careful substrate cleaning is necessary to reach good adhesion of deposits. The bond-coats may also improve the *intrinsic adhesion* of films very different from the substrate. Especially, the hard and wear-resistant diamond-like films require intermediate films to improve their adhesion to metallic substrates. Consequently, Ti bond-coat was applied to improve adhesion of *DLC* films to steel substrates [79]. The adhesion of such films to Al substrate was improved by adding a small quantity of aluminum atoms to the graphite target used for deposition. These atoms sputtered together with carbon ones forming a very thin intermediate layer resulting in stronger adhesion [80].

The methods of surface activation depend on the activated substrate material and are realized using liquids, photons, and large (sand) or small particles (molecules, atoms, and ions).

1.5.1.1 Liquids Activation

Liquids are frequently applied for substrate cleaning by chemical etching[10] in semiconductor industry. The GaAs wafers were cleaned up with some acids before the $(NH_4)_2S$ solution was applied. This solution enabled sulfidation of surface and avoidance of oxidation prior to the application of metallic layers [81]. The chemical treatment using HF solution was one of the methods applied to prepare Si substrate before deposition of Al_2O_3 thin film by atomic film deposition (*ALD*) method [82]. The same acid was a part of WC-Co substrate surface activation prior to deposition of *DLC* film by *CVD* method [83].

1.5.1.2 Photons Activation

The laser may activate the surface by evaporation of impurities and modification of its morphology. This activation is called laser surface texturing (*LST*). An example of such texturing including formation of dimples, crossed grooves, and concentric rings obtained on an aluminum alloy substrate using Nd: YVO_4 picosecond laser is shown respectively in Fig. 1.16a–d.

Table 1.14 shows a few examples of surfaces activation using *LST*. Such texturing can be made with *cw* laser, which heats up the surface. The heating may evaporate a lower melting point part of composite such as cobalt in WC-Co [85].

Another possible action is evaporation of small holes in thermoplastic polymer by short laser pulses. Such texturing enabled increase in the adhesion strength of evaporated aluminum coatings to *PEEK* from 0.7 to 5.5 MPa [86]. Finally, an appropriate pulsed laser texturing enables reaching the density of diamond clusters nucleation equal to about 5.3×10^7 clusters/cm^2 [87].

1.5.1.3 Particles Activation

Activation using coarse particles such as sand is a method used frequently as a pretreatment prior to granular coatings. Some authors used it however to prepare substrate before deposition of thin films. In particular, Zhang and Zhou [83] used sand-blasting to treat hard WC+ 6 wt. % Co substrate prior of *CVD* deposition of a *DLC* film and Grubova et al. [88] applied sand to blast on Ti-substrate prior to the deposition of Ag-doped *HA* by sputtering. It must be added that the sand-blasting was followed in cited studies by acid etching to complete the substrate activation.

The atomic-size species, i.e. ions, atoms, and molecules, are used frequently to activate surface. The species are part of plasma, and their energy of ions at treatment depends mainly on gas pressure and acceleration voltage. Some examples of atomic-size species treatment are shown in Table 1.15.

---

10 See also Section 1.3.1 of this chapter

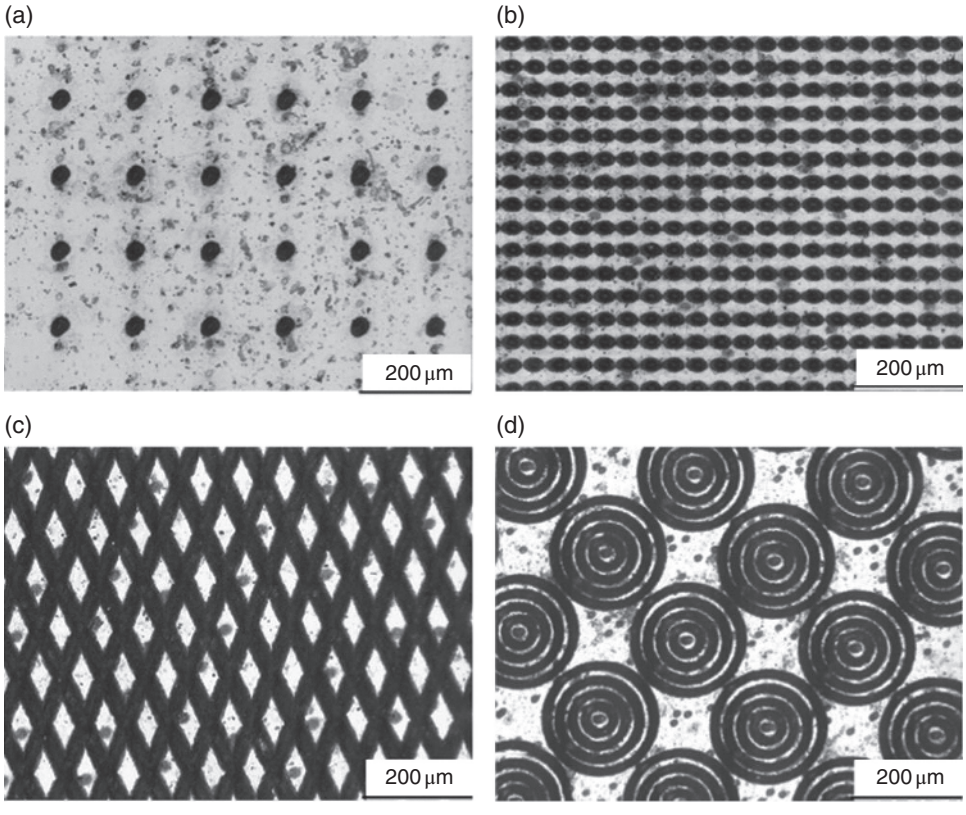

Figure 1.16 Optical micrographs of laser-treated surface of aluminum alloy (Alloy AA2024-T3 of Al + (3.8–4.9) wt. % Cu + (1.2–1.8) wt. % Mg) textured using Nd: YVO_4 picosecond laser ($\lambda = 1064$ nm) showing different densities of dimples (a, b), crossed grooves (c), and concentric rings (d). *Source:* From Min et al. [84]/Reproduced with permission from ELSEVIER.

The *i-beam* pretreatment renders possible the chemical reaction in the interface between film and substrate. Gheriani et al. [89] reported about formation of carbides such as Cr_7C_3 between steel substrate and Cr film. This reaction occurred after high-temperature annealing of coated samples rendering possible diffusion of small C atoms in in Cr film. The choice of ions and their energy used to the treatment must be adapted to the substrate material [90, 91]. Consequently, the application of heavier Xe^+ ions activated better the surface of polymers than Ar^+ and, on the other hand, the highest bias voltage of $U = -600$ V was most favorable for adhesion of *DLC* films to steel substrate.

Plasma treatment is useful for activation of polymers' surface. Corona discharge is frequently used in this process. The discharge, done in open atmosphere, breaks the polymer chains and creates the radicals [93]. The treatment using arc plasma torch also improved the adhesion of Al films to *PE* and *PEEK* polymers [86]. Finally, a plasma generated under vacuum by a high-voltage pulse (up to $U = -15$ kV) in presence of different gases such as C_2H_4, N_2, or O_2 enabled to activate Cu substrate surface and render possible the deposition of *DLC* films [92].

Table 1.14 Examples of different substrates activated prior to atomistic film deposition using laser surface texturing.

Laser	Wavelength, nm	Substrate material	Film material	Method of film deposition	Final application	Remarks	Reference
Diode laser *cw*	940	WC + 6 wt. % Co	Polycrystalline diamond	*HFCVD*	Wear-resistant films	Co-binder was removed	[85]
Nanosecond laser[a]	355	Thermoplastic polymers: *PP*, *PEEK,* and *PE*	Al	Evaporation	Automotive, aerospace, and medical applications	Square grid pattern was textured	[86]
Nd: YAG nanosecond	1064	Nb	Boron-doped diamond	*HFCVD*	Waste water treatment electrodes	Laser spot has diameter of about 30 μm	[87]

[a] Laser type was not precised in the paper. The lasers Nd: YAG, diode, or fiber emit this wavelength.

Table 1.15 Examples of surface activation prior to atomistic film deposition using species having atomic sizes.

Method of treatment	Pressure at treatment, Pa	Substrate material	Film material	Method of film deposition	Final application	Remarks	Reference
Activation by ions	10	Steel 100C6	Cr	Sputtering	Wear-resistant films	Ar^+ ion treatment improved films adhesion and their microhardness	[89]
	—	Polymers as *PC*	HfO_2 or ZrO_2		Optical antireflection coatings	Ions Ar^+ and Xe^+	[90]
	11	Stainless steel 304	*DLC*	*PECVD*	Wear-resistant films	Ions Ar^+ accelerated by voltage up to 600V	[91]
Plasma	0.7	Cu		Ion implantation		Preimplantation using N_2 and O_2, Ar, CO_2, and C_2H_4	[92]
	10^5	Thermoplastic polymers: *PP*, *PEEK*, and *PE*	Al	Evaporation	Automotive, aerospace, and medical applications	Arc-generated air plasma	[86]

1.5.2 Activation of the Substrates Before Granular Deposits

The granular deposits grow up starting from molten particles, which impact the substrate's surface. The size of particles varies from sub-micrometers occurring in the methods of spraying using liquid feedstock such as solution precursor plasma spraying (*SPPS*), suspension plasma spraying (*SPS*) or spray pyrolysis (*SP*) up to many tenths of micrometers in the methods using solid feedstock such as atmospheric plasma spraying (*APS*), cold-gas spraying method (*CGSM*), or arc spraying (*AS*). The liquid droplets are transformed into splats. The size and shape of solidified splats depend on their velocity at impact and on the topography and temperature of surface [74, 94]. The topography of the surface and, in particular, its roughness are essential in the mechanism of adhesion called ***mechanical anchorage***. The methods of activation modify this topography. The description of this modification is generally related to the roughness. However, the laser surface texturing (*LST*), which is at present intensively researched as activation method, enables more precise description of the holes array generated by laser [95]. The final result of activation is the improvement of coatings adhesion. The adhesion is generally characterized using standard tensile strength test ASTM C633–01[11].

1.5.2.1 Particles Activation

The substrates for granular deposits are activated mainly by grit-blasting. The method consists of accelerating the particles of hard material (corundum, hard steel, silica, silicon carbide) in a jet of compressed air. The ceramic particles have generally angular shape, and the metallic ones sometimes are spherical. The particles bombard the surface of a substrate making it rough. The industrial installations are equipped in several simultaneously acting nozzles being controlled numerically controlled automata. The main blasting parameters are shown in Table 1.16.

The grit particle size used in blasting depends on the thickness of the workpiece (fine grit is recommended for thin deposits) and the desired surface roughness of final deposit (fine grit blasting renders the surface smoother). Roseberry and Boulger [96] made the recommendations of grit size for the plasma-sprayed coatings of different thicknesses. Consequently, silica grit is often used for thin coatings applied without polishing, while alumina is used as a coarse one.

The grit's size determines the roughness of the treated surface. Mellali et al. [97, 98] analyzed substrates of different elasticity and found that the roughness after grit-blasting is lower for the substrate having greater elasticity modulus. Similarly, Wigren [99] after having studied different metals and alloys blasted with alumina grit found that the R_a parameter decreases linearly from 4.5 to 2.5 μm with the substrate's modulus of elasticity increasing from 40 GPa (Mg) to 240 GPa (Co-based Haynes 188 alloy composed of Co + 22 wt.% Ni + 22 wt. % Cr + 13 wt. % W + 3 wt. % Fe). Finally, grit blasting generates compression stresses in the substrate, and thin substrates can deform after blasting.

11 Standard Test Method for Adhesion and Cohesion of Thermal Sprayed Coatings of 10 March 2001

Table 1.16 Principal grit-blasting parameters.

Process element	Parameters
Grit	Material, particle size, hardness
Activated surface	*Young's* modulus, geometric dimension (size and thickness), hardness
Grit-blasting medium	Compressed air
Blasting set-up	Blasting in a booth or in open atmosphere
Technique of blasting	Processing time, air pressure, blasting distance

The research on the influence of grit-blasting parameters and on the surface roughness R_a or on the *intrinsic adhesion* of deposits to the substrate may be summarized in the following way:

- roughness, characterized by R_a:
  - reaches a maximum after some blasting time;
  - increases with the blasting pressure;
  - is not strongly influenced by blasting distance between nozzle and substrate;
- the grit blasting angle[12] may influence the roughness and the adhesion:

It is important to mention that the grit particles may get embedded in the treated surface. This embedment may decrease the adhesion of the coating. Subsequently, embedment is a major disadvantage of activation by grit blasting.

The *dry-ice* (solid CO_2) blasting enables avoiding embedment. The solid CO_2 sublimes without forming liquid phase and was applied *in situ* to activate Ti6Al4V (Ti + 6 wt. % Al + 4 wt. % V) alloy during spraying hydroxyapatite (*HA*) [100]. The roughness, R_a, of sprayed deposit was slightly smaller at *dry-ice* treatment ($R_a = 8\,\mu m$) than after pre-treatment using alumina sand blasting ($R_a = 12\,\mu m$). The bond strength of as-sprayed coatings increased however up to 55 MPa comparing to 22 MPa in samples prepared using sand-blasting.

1.5.2.2 Photons Activation

The laser surface texturing (*LST*) activation of substrates prior to granular coating deposition has been intensively researched in recent years. The authors drilled holes using different lasers in the substrate in the way shown in Fig. 1.16a and defined the geometry-treated surface by giving following parameters:

- distance between the holes, being generally equal in x and y directions;
- diameter and depth of the holes;
- angle of the hole axis (being angle of laser treatment) with regard to the normal to surface.

12 The blasting angle of 0° corresponds to the direction normal to the surface

The diameters of the holes are comparable to the estimated size of liquid droplets arriving on the substrate. Otherwise, the droplets cannot penetrate into the holes. Similarly, the angle of laser treatment increases the hole diameter as found by Kromer et al. [95] for the Al substrate drilled using pulsed Nd: YAG laser.

The description of different coating and different deposition methods obtained by *LST* pre-treatment are mentioned in Table 1.17. All authors used pulsed fiber laser and optimized the texturing geometry. The adhesion of coating deposited onto substrates textured using optimization improved considerably compared to other pretreatment methods. Kromer et al. [95] mentioned that for some *LST* conditions the adhesion strength was greater than coating cohesion. Texturing may modify the mechanical properties of substrate. The modification of microhardness was observed close to surface of aluminum alloy Al2017 submitted to texturing using pulsed fiber laser [103].

The lasers may be used *in situ*, i.e. during coating deposition. Two different Nd: YAG pulsed laser were used simultaneously to clean up and to heat up the substrate immediately before the plasma torch arrived at the treated area. However, the adhesion NiAl coatings to Al-alloy and Ti-alloy substrate decrease compared to grit-blasting pre-treatment, due to the decrease of surface roughness [104]. Finally, the shape of the laser-drilled holes at *LST* can be modified by 2-step processing. The first step enables holes drilling and the second one smoothens the surface and lowers its roughness. Such pre-treatment was made using nanosecond pulsed fiber laser, and the different laser fluences and scans velocities enabled 2 steps to be realized [105].

1.5.2.3 Water jet Activation

The treatment with a water jet does not have this drawback, but it is not yet used often in the industry. The research studies of Taylor and Knapp [106, 107], related to water jet treatment of Inconel alloys, enabled to find the essential parameters of this treatment (see Table 1.18).

The results of research show that the surface of alloy Inconel 718 starts to be rough at water pressure of $p = 200$ MPa. The interface between the plasma-sprayed MCrAlY coating and the substrate was perfectly clean compared to grit-blasted sample surface. Finally, the adhesion strength was between 70 and 80 MPa for coatings on substrates treated with water jet compared to the values of 46–78 MPa for coatings on the grit-blasted substrates.

1.5.2.4 Plasma Activation

Plasma treatment such as cleaning and activation can be realized under vacuum or under inert gas atmosphere. The realization of such pre-treatment in air may lead to the metal surface oxidation. Takeda and Takeuchi [108] studied pre-treatment using arc under vacuum. The authors focused on the cleaning of oxides from stainless steel substrate, which may be useful prior to vacuum plasma spraying (*VPS*). More recently, Lukauskaite et al. [109] used cathodic treatment prior to *APS*. The treatment was realized under protecting Ar in open atmosphere to activate and clean up aluminum alloy plates to be coated with NiAl. The final coatings' adhesion strength improved from 23 MPa for grit-blasted samples up to 32 MPa for cathodically treated ones.

Table 1.17 Examples of different substrates activated prior to granular coatings deposition using laser surface texturing.

Laser	Wavelength and pulse duration	Substrate	Geometry of textured array[a]	Initial powder and its size, μm	Method of coatings deposition	Final application	Remarks	Reference
Fiber laser	1064 nm 100 ns	Al 2017 alloy, Al + 4 wt. % Cu + Si, Mn, Fe	$D = 60\,\mu m$, $x = 100$, 150, 200 and 300, $L = 80\,\mu m$, $\alpha = 0$ and 30°	Ni + 5 wt. % Al, $d_{50} = 67\,\mu m$	*APS*	Bond-coat	Adhesion strength 34–52 MPa	[95]
		Steel ASTM 1045	$D = 40$–$120\,\mu m$, $x = 30$–$110\,\mu m$, $L = 50\,\mu m$	Ni60 alloy, Ni + 16 wt. % Cr + 9 wt. % Fe + 4 wt. % Si			Adhesion strength up to 50 MPa for $x = 30\,\mu m$	[101]
		Al alloy 7000, Mg alloy RZ6, Al + 20 vol. % SiC	$D = 50\,\mu m$, $x = 80$ and $150\,\mu m$, $L = 25\,\mu m$	Al alloy 6000, Mg alloy, and Al + 20 vol. % SiC, $d_{50} = 40\,\mu m$	*CGSM*	Light metal coating	Adhesion up to 50 MPa for Al-alloy	[102]
		Thermoset carbon fiber composite	$D = 50\,\mu m$, $x = 200$ and $300\,\mu m$, $L = 25\,\mu m$	Cu_05T wire	*AS*	Metallization	Adhesion up to 13 MPa	
		AM1 single crystal, Ni + Cr,Co, Ta, W, Al, Mo, Ti	$D = 60$ and $80\,\mu m$, $x = 100$ and $150\,\mu m$, $L = 40\,\mu m$	$ZrO_2 + 7$ wt. % Y_2O_3	*APS*	*TBC*	Adhesion up to 33 MPa	

[a] D is diameter of hole, x is the distance between holes' centers, L is their depth, and α is angle of between hole axis and normal to the surface.

Table 1.18 Typical parameters of surface activation using a water jet.

Parameter	Value
Water pressure, MPa	200–350
Water flow rate, L/min	3.5–4.5
Nozzle *ID*, mm	0.4
Distance between nozzle and substrate, cm	8
Scan speed of water jet, cm/min	30–130
Width of the trace of treatment in the substrate, mm	1.5
Shift of following traces, mm	0.8

Source: Adapted from Taylor [106].

References

1 Mattox, D.M. (1982). Adhesion and surface preparation. In: *Deposition Technologies for Films and Coatings* (ed. R.F. Bunshah), 63–82. Park Ridge, NJ: Noyes Publications.
2 Metev, S.M. and Veiko, V.P. (1998). *Laser-Assisted Microtechnology*, 2e. Berlin: Springer.
3 Burakowski, T. and Wierzchoń, T. (1995). *Surface Engineering of Metals*. Warsaw: WNT (in Polish).
4 Kingery, W.D., Bowen, H.K., and Uhlmann, D.R. (1976). *Introduction to Ceramics*, 2e. New York, NY: Wiley.
5 Wand, J. and Guo, X. (2020). Adsorption isotherm models: classification, physical meaning, application and solving method. *Chemosphere* 258: 127279.
6 Elder, S.H., DiSalvo, F.J., Topor, L., and Navrotsky, A. (1993). Thermodynamics of ternary nitride formation by ammonolysis: application to $LiMoN_2$, Na_3WN_3 and Na_3WO_3N. *Chem. Mater.* 5 (10): 1545–1553.
7 Ashby, M.F. and Jones, D.R.H. (1991). *Matériaux, Tome 1*. Paris: Dunod (in French).
8 Callister, W.D. Jr. (1994). *Materials Science and Engineering: An Introduction*, 3e. New York, NY: Wiley.
9 Lide, D.R. (ed.) (1997). *CRC Handbook of Chemistry and Physics*, 78e. Boca Raton, FL: CRC Press.
10 Frommeyer, G., Rablbauer, R., and Schäfer, H.J. (2010). Elastic properties of B2-ordered NiAl and NiAl-X (Cr,Mo,W) alloys. *Intermetallics* 18 (3): 299–305.
11 Technical Data of catalogue Delloro Stellite, Cheney Manor Industrial Estate, Swindon SN2 2PW, UK, 2008.
12 The Engineering ToolBox available on https://www.engineeringtoolbox.com/young-modulus-d_417.html checked on 18 September 2024.
13 Ashby, M.F. and Jones, D.R.H. (1991). *Matériaux, Tome 2*. Paris: Dunod (in French).
14 Dörre, E. and Hübner, H. (1984). *Alumina*. Berlin: Springer.
15 Pawłowski, L. and Blanchart, P. (2018). *Industrial Chemistry of Oxides for Emerging Applications*. Chichester: Wiley.
16 Samsonov, G.V. (ed.) (1978). *Physical and Chemical Properties of Oxides*. Moskva, USSR: Metallurgija (in Russian).

17 Snustad, I., Roe, I.T., Brunsvold, A. et al. (2018). A review on wetting and water condensation - perspectives for CO_2 condensation. *Adv. Colloid Interf. Sci.* 256: 291–304.

18 Eustathopoulos, N., Nicholas, M.G., and Drevet, B. (1999). *Wettability at High Temperatures*. Kidlington, Oxford: Pergamon Press and Elsevier Science.

19 Carr, J., Milhet, X., Gadaud, P. et al. (2015). Quantitative characterization of porosity and determination of elastic modulus for sintered micro-silver joints. *J. Mater. Process. Technol.* 225: 19–23.

20 Klein, C.A. and Cardinale, G.F. (1993). Young's modulus and poisson's ratio of CVD diamond. *Diam. Relat. Mater.* 2: 918–923.

21 Callister, W.D. and Rethwisch, D.G. (2008). *Fundamentals of Materials Science and Engineering*, 3e. New York, NY: Wiley.

22 Stachurski, Z. (1987). *Engineering Science of Polymeric Materials*. Parkville, VIC: Polymer Division, Royal Australian Chemical Institute.

23 Wyatt, O.H. and Dew-Hughes, D. (1978). *Metals, Ceramics and Polymers*. Warsaw: PWN (In Polish).

24 Seidel, W.W. and Hahn, F. (2014). *Werkstofftechnik*, 10e. Munich: Hanser.

25 Małachowska, A. (2015). *Analysis of the cold gas spraying process and determination of selected properties of metallic and cermet coatings*. PhD Thesis. University of Limoges and Wrocław University of Technology.

26 Mercier, J.P. and Maréchal, E. (1996). *Chimie de Polymères: Synthèses, Réactions, Dégradation*. Lausanne: PPUR (In French).

27 Mattox, D.M. (1994). Surface preparation for film and coating deposition processes. In: *Handbook of Deposition Technologies for Films and Coatings*, 2e (ed. R.F. Bunshah), 82–126. Park Ridge, NJ: Noyes Publications.

28 Sonoda, T., Watazu, A., Zhu, J. et al. (2001). A surface cleaning method for sputter deposition of pure titanium film onto TiNi shape memory alloy substrate. *Vacuum* 60 (1–2): 197–199.

29 Kratz, F., Grass, S., Umanskaya, N. et al. (2015). Cleaning of biomaterial surfaces: protein removal by different solvents. *Colloids Surf. B: Biointerfaces* 128: 28–35.

30 Buck, V. and Deuerler, F. (1998). Enhanced nucleation of diamond films on pretreated substrates. *Diam. Relat. Mater.* 7: 1544–1552.

31 Zhang, Z.M., He, X.C., Shen, H.S. et al. (2000). Pretreatment for diamond coatings on free-shape WC-Co tools. *Diam. Relat. Mater.* 9: 1749–1752.

32 Shen, M.R., Wang, H., Ning, Z.Y. et al. (1997). Enhanced diamond nucleation on pretreated silicon substrates. *Thin Solid Films* 301: 77–81.

33 Couillard, J.G., Ast, D.G., Umbach, C. et al. (1997). Chemical treatment of glass substrates. *J. Non-Cryst. Solids* 222: 429–434.

34 Lubna, H., Auner, G., Patwa, R. et al. (2011). Role of cleaning methods on bond quality of Ti coated glass/imidex system. *Appl. Surf. Sci.* 257: 4749–4753.

35 Cooper, K., Gupta, A., and Beaudoin, S. (2001). Simulation of the adhesion of particles to surfaces. *J. Colloid Interface Sci.* 234: 284–292.

36 Thornton, J.A. and Greene, J.E. (1994). Plasma in deposition processes. In: *Handbook of Deposition Technologies for Films and Coatings*, 2e (ed. R.F. Bunshah), 29–77. Park Ridge, NJ: Noyes Publications.

37 Rossnagel, S.M. (1991). Glow discharge plasma and sources for etching and deposition. In: *Thin Film Processes II* (ed. J.L. Vossen and W. Kern), 11–76. San Diego, CA: Academic Press.

38 Mézerette, D., Belmonte, T., Hugon, R. et al. (2001). Surface cleaning and passivation of an iron foil by a nitrogen post-discharge surface treatment. *Surf. Coat. Technol.* 142–144: 761–766.

39 Mattox, D.M. (1998). *Handbook of Physical Vapor Deposition (PVD) Processing*. Westwood, NJ: Noyes Publications.

40 Zelm, P.C. (1985). Elementary processes in plasma-surface interaction with emphasis on ions. *Pure Appl. Chem.* 57 (9): 1253–1264.

41 Ochs, D., Schroeder, J., Cord, B., and Scherer, J. (2001). Glass substrate cleaning at low energy ion source. *Surf. Coat. Technol.* 142–144: 767–770.

42 Goto, T., Takekawa, S., Moriya, M. et al. (2000). Growth of a-axis oriented $YBa_2Cu_3O7_{-\delta}$ films on ion-beam cleaned $LaSrGaO_4$ substrates. *Physica C* 341–348: 2373–2374.

43 Curran, J.E. (1983). The use of plasmas to deposit and etch materials. *Phys. Technol.* 14: 283–296.

44 Jundale V.A., Chorage G.Y. and Yadav A.A. Structural, morphological and optical properties of $CoFe_2O_4$ thin film by spray pyrolysis technique. *Materials Today: Proceedings*, in press, doi.org/10.1016/j.matpr.2020.05.077.

45 Loosen, P. and Treusch, H.-G. (1993). Laserstrahlquellen für industrielle Fertigungstechnik. In: *Werkstoffbearbeitung Mit Laserstrahlung* (ed. G. Herzigen and P. Loosen). Munich: Carl Hanser Verlag (in German).

46 Reitz, W. (1998). Surface cleaning and coating removal with lasers. In: *Lasers in Surface Engineering* (ed. N.B. Dahotre). Materials Park, OH: ASM International.

47 Pawłowski, L. (1999). Thick laser coatings: a review. *J. Thermal Spray Technol.* 8 (2): 279–295.

48 Lu, Y.F., Song, W.D., and Hong, M.H. (1996). Laser removal of particles from magnetic head sliders. *J. Appl. Phys.* 80 (1): 499–504.

49 Turner, M.W., Crouse, P.L., Li, L., and Smith, A.J.E. (2006). Investigation into CO_2 laser cleaning of titanium alloys for gas-turbine component manufacture. *Appl. Surf. Sci.* 252 (13): 4798–4802.

50 Turner, M.W., Crouse, P.L., and Li, L. (2006). Comparison of mechanisms and effects of Nd:YAG and CO_2 laser cleaning of titanium alloys. *Appl. Surf. Sci.* 252 (13): 4792–4797.

51 Raza, M.S., Das, S.S., Tudu, P., and Saha, P. (2019). Excimer laser cleaning of black sulphur encrustation from silver surface. *Opt. Laser Technol.* 113: 95–103.

52 Schmidt, M.J.J., Li, L., and Spencer, J.T. (1999). Characteristics of high power diode laser removal of multilayer chlorinated rubber coatings from concrete surfaces. *Opt. Laser Technol.* 31: 171–180.

53 Tian, Z., Lei, Z., Chen, X. et al. (2020). Nanosecond pulsed fiber laser cleaning of natural marine micro-biofoulings from the surface of aluminum alloy. *J. Clean. Prod.* 244: 118724.

54 Razaba, M.K.A.A., Noor, A.M., Jaafar, M.S. et al. (2018). A review of incorporating Nd:YAG laser cleaning principal in automotive industry. *J. Radiat. Res. Appl. Sci.* 11: 393–402.

55 Dupuis, P., Cormier, Y., Fenech, M. et al. (2016). Flow structure identification and analysis in fin arrays produced by cold spray additive manufacturing. *Int. J. Heat Mass Transf.* 93: 301–313.

56 Randall, J.N., Owen, J.H.G., Fuchs, E. et al. (2018). Digital atomic scale fabrication an inverse Moore's Law – a path to atomically precise manufacturing. *Micro and Nano Engineering* 1: 1–14.

57 Köhler, M. and Fritzsche, W. (2004). *Nanotechnology. An introduction to Nanostructuring Techniques*. Weinheim: Wiley-VCH.

58 Mayer, T.M. and Allen, S.D. (1991). Selected area processing. In: *Thin Film Processes II* (ed. J.L. Vossen and W. Kern), 622–667. San Diego, CA: Academic Press.

59 Sebastian, E.M., Jain, S.K., Purohit, R. et al. (2020). Nanolithography and its current advancements. *Materials Today: Proceedings* 26: 2351–2356.

60 Bliznetsov, V., Kumar, R., Lin, H. et al. (2006). Integrated process of photoresist trimming and dielectric hard mask etching for sub-50 nm gate patterning. *Thin Solid Films* 504: 117–120.

61 Lipson, S.G. (2003). Why is super-resolution so inefficient? *Micron* 34 (6–7): 309–312.

62 RP Photonics Encyclopedia, https://www.rp-photonics.com/numerical_aperture.html (accessed 4 January 2021).

63 Dreeskornfeld, L., Hainl, G., Kleinberg, U. et al. (2004). Nanostructuring of Mo/Si multilayers by means of reactive ion etching using three- level mask. *Thin Solid Films* 458: 227–232.

64 Jantawong, J., Atthi, N., Leepattarapongpan, C. et al. (2019). Fabrication of MEMS-based capacitive silicon microphone structure with staircase contour cavity using multi-film thickness mask. *Microelectron. Eng.* 206: 17–24.

65 Huang, H.-W., Kao, C.-C., Hsueh, T.-H. et al. (2004). Fabrication of GaN-based nanorod LED using self-assemble nickel nano-mask and ICP reactive ion etching. *Mater. Sci. Eng. B* 113: 125–129.

66 Fonseca Filho, H.D., Maricio, M.H.P., Ponciano, C.R., and Prioli, R. (2004). Metal layer mask patterning by force microscope lithography. *Mater. Sci. Eng. B* 112: 194–199.

67 Luo, J., Zheng, H., Chen, W. et al. (2019). Conical-shaped hexagonal barium ferrite nanodot arrays on an alumina substrate based on an ultrathin alumina mask method. *J. Magn. Magn. Mater.* 489: 165449.

68 Wagner, E., Sandu, C.S., Harada, S. et al. (2015). Fabrication of complex oxide microstructures by combinatorial chemical bean vapor deposition through stencil masks. *Thin Solid Films* 586: 64–69.

69 Park, S.J., Kim, D., Lee, S. et al. (2018). Diamond-like amorphous carbon layer film by an ICP system for next generation etching hard mask. *Thin Solid Films* 663: 21–24.

70 Liu, H.W., Gao, C.X., LI, X. et al. (2001). Selective deposition of diamond films on insulators by selective seeding with a double –layer mask. *Diam. Relat. Mater.* 10: 1573–1577.

71 Ashby, C.I.H. (1991). Laser-driven etching. In: *Thin Film Processes II* (ed. J.L. Vossen and W. Kern), 783–846. San Diego, CA: Academic Press.

72 Chen, H.-Y., Han, D., Tian, Y. et al. (2014). Mask-free and programmable patterning of graphene by ultrafast direct writing. *Chem. Phys.* 430: 13–17.

73 Drabik, M., Truchly, M., Ballo, V. et al. (2018). Influence of substrate material and its plasma pretreatment on adhesion and properties of WC/a-C:H nanocomposite coatings deposited at low temperature. *Surf. Coat. Technol.* 333: 138–147.

74 Pawłowski, L. (2008). *The Science and Engineering of Thermal Spray Coatings*. Chichester: Wiley.

75 Oukach, S., Pateyron, B., and Pawłowski, L. (2019). Physical and chemical phenomena occurring between solid ceramics and liquid metals and alloys at laser and plasma composite coatings formation: a review. *Surf. Sci. Rep.* 74 (3): 213–241.

76 Abermann, R. (1990). Internal stress of vapor- deposited aluminum on aluminum substrate films: effect of O_2 and water incorporated in the substrate. *Thin Solid Films* 188: 385–394.

77 Poppeller, M. and Abermann, R. (1997). Influence of substrate properties on the growth of titanium films. Part I. *Thin Solid Films* 295: 60–66.

78 Oberhauser, R. and Abermann, R. (1999). Influence of substrate properties on the growth of titanium films. Part III. *Thin Solid Films* 350: 59–66.

79 Voevodin, A.A. and Zabinski, J.S. (1998). Superhard, functionally gradient, nanolayered and nanocomposite diamond-like carbon coatings for wear protection. *Diam. Relat. Mater.* 7: 463–467.

80 Sasaki, Y., Nose, K., Kamiko, M., and Mitsuda, Y. (2011). High adhesion of diamond-like carbon thin film to aluminum alloy achieved by substrate sputtering and redeposition method. *Surf. Coat. Technol.* 206: 143–148.

81 Kang, M.-G. and Park, H.H. (2002). Surface preparation and effective contact formation for GaAs surface. *Vacuum* 67: 91–100.

82 Chang, Y., Ducroquet, F., Gautier, E. et al. (2004). Surface preparation and post thermal treatment effects on interface properties of thin Al_2O_3 films deposited by ALD. *Microelectron. Eng.* 72: 326–331.

83 Zhang, B. and Zhou, L. (1997). Effect of sandblasting on adhesion strength of diamond coatings. *Thin Solid Films* 307: 21–28.

84 Min, J., Wan, H., Carlson, B.E. et al. (2020). Application of laser ablation in adhesive bonding of metallic materials: a review. *Opt. Laser Technol.* 128: 16188.

85 Barletta, M., Rubino, G., and Gisario, A. (2011). Adhesion and wear resistance of diamond coatings laser treated WC-Co substrates. *Wear* 271: 2016–2024.

86 Knapp, W., Djomani, D., Coulon, J.F., and Grunchec, R. (2014). Influence of structuring by laser and plasma torch on the adhesion of metallic films on thermoplastic substrates. *Phys. Procedia* 56: 791–800.

87 Xu, C., Xu, F., Shi, L. et al. (2019). Enhancement of substrate-coating adherence of boron-doped diamond electrodes by nanosecond laser surface texturing pretreatment. *Surf. Coat. Technol.* 360: 196–204.

88 Grubova, I.Y., Surmeneva, M.A., Ivanova, A.A. et al. (2015). The effect of patterned titanium substrates on the properties of silver-doped hydroxyapatite coatings. *Surf. Coat. Technol.* 276: 595–601.

89 Gheriani, R., Halimi, R., and Bensaha, R. (2004). Effect of substrate surface ion bombardment etching on reaction between chromium thin films and steel substrates. *Surf. Coat. Technol.* 180–181: 49–52.

90 Sarto, F., Alvisi, M., Melissano, E. et al. (1999). Adhesion enhancement of optical coatings on plastic substrate via ion treatment. *Thin Solid Films* 346: 196–201.

91 Jones, B.J., Anguilano, L., and Ojeda, J.J. (2011). Argon plasma treatment techniques on steel and effects on DLC structure and delamination. *Diam. Relat. Mater.* 20: 1030–1035.

92 Flege, S., Hatada, R., Ensinger, W., and Baba, K. (2014). Improved adhesion of DLC films on copper substrates by preimplantation. *Surf. Coat. Technol.* 256: 37–40.

93 Goldman, M., Goldman, A., and Sigmond, R.S. (1985). The corona discharge, its properties and specific uses. *Pure Appl. Chem.* 57 (9): 1353–1362.

94 Danlos, Y., Costil, S., Liao, H., and Coddet, C. (2008). Combining effects of ablation laser and laser preheating on metallic substrates before thermal spraying. *Surf. Coat. Technol.* 202: 4531–4537.

95 Kromer, R., Costil, S., Cormier, J. et al. (2015). Laser surface patterning to enhance adhesion of plasma sprayed coatings. *Surf. Coat. Technol.* 278: 171–182.

96 Roseberry, T.J. and Boulger, F.W. (1977). *A Plasma Flame Spray Handbook*, Rapport no. MT – 043. Springfield, VA: U. S. Department of Commerce, National Technical Information Center.

97 Mellali, M., Grimaud, A., and Fauchais, P. (1994). Parameters controlling the sand blasting of substrates for plasma spraying. In: *Thermal Spray Industrial Applications* (ed. C.C. Berndt and S. Sampath), 227–232. Materials Park, OH: ASM International.

98 Mellali, M., Fauchais, P., and Grimaud, A. (1996). Influence of substrate roughness and temperature on the adhesion/cohesion of alumina coatings. *Surf. Coat. Technol.* 81: 275–286.

99 Wigren, J. (1988). Grit blasting as surface preparation before plasma spraying. In: *Thermal Spray: Advances in Coatings Technology* (ed. D.L. Houck), 99–104. Materials Park, OH.

100 Dong, S., Zeng, J., Li, L. et al. (2017). Significance of in-situ dry-ice blasting on the microstructure, crystallinity and bonding strength of plasma-sprayed hydroxyapatite coatings. *J. Mech. Behav. Biomed. Mater.* 71: 136–147.

101 Tan, N., Xing, Z.-G., Wang, X.-L. et al. (2017). Deposition mechanism of plasma sprayed droplets on textured surfaces with different diameter-to-distance ratios. *Mater. Des.* 133: 19–29.

102 Kromer, S., Costil, S., Verdy, C. et al. (2018). Laser surface texturing to enhance bond strength of spray coatings – cold spraying, wire-arc spraying, and atmospheric plasma spraying. *Surf. Coat. Technol.* 352: 642–653.

103 Costil, S., Lamraoui, A., Langlade, C. et al. (2014). Surface modifications induced by pulsed-laser texturing. Influence of laser impact on the surface properties. *Appl. Surf. Sci.* 288: 542–549.

104 Danlos, Y., Costil, S., Liao, H., and Coddet, C. (2011). Influence of Ti-6Al-4V and Al 2017 substrate morphology on Ni-Al coating adhesion. Impact of laser treatment. *Surf. Coat. Technol.* 205: 2702–2708.

105 Gao, Y., Wu, B., Zhou, Y., and Tao, S. (2011). A two-step nanosecond laser surface texturing process with smooth surface finish. *Appl. Surf. Sci.* 257: 9960–9967.

106 Taylor, T.A. (1995). Surface roughening of metallic substrates by high pressure pure waterjet. *Surf. Coat. Technol.* 76–77: 95–100.

107 Knapp, J.K. and Taylor, T.A. (1996). Waterjet surface analysis and bond strength. *Surf. Coat. Technol.* 86–87: 22–27.

108 Takeda, K. and Takeuchi, S. (1997). Removal of oxide layer on metal surface by vacuum arc. *Mater. Trans. Jap. Inst. Metals* 38 (7): 636–642.

109 Lukauskaite, R., Cernasejus, O., Skamat, J. et al. (2017). The effect of Al-Mg substrate preparation on the adhesion strength of plasma sprayed Ni-Al coatings. *Surf. Coat. Technol.* 316: 93–103.